Heat Transfer Analysis of Viscoelastic Fluid Flow in a Peripheral Layer

By

Mehwish

Registration No: 833-FBAS/MSMA/F22

Department of Mathematics & Statistics
Faculty of Sciences
International Islamic University, Islamabad
Pakistan

2024

Heat Transfer Analysis of Viscoelastic Fluid Flow in a Peripheral Layer

By

Mehwish

Registration No: 833-FBAS/MSMA/F22

Supervised by

Dr. Khadija Maqbool

Department of Mathematics & Statistics
Faculty of Sciences
International Islamic University, Islamabad
Pakistan

2024

Heat Transfer Analysis of Viscoelastic Fluid Flow in a Peripheral Layer

By

Mehwish

Registration No: 833-FBAS/MSMA/F22

A Thesis
Submitted in the Partial Fulfillment of the
Requirement for the Degree of
MASTER OF SCIENCE
In
MATHEMATICS

Supervised by

Dr. Khadija Maqbool

Department of Mathematics & Statistics
Faculty of Sciences
International Islamic University, Islamabad
Pakistan

2024

<u>Certificate</u>

Heat Transfer Analysis of Viscoelastic Fluid Flow in a Peripheral Layer

By

Mehwish

A DISSERTATION SUBMITTED IN THE PARTIAL FULFILLMENT

OF THE

REQUIREMENTS FORTHE DEGREE OF MASTER OF SCIENCE

IN MATHEMATICS

We accept this thesis as conforming to the required standard

1.__________________ 2. ____________________

Prof. Dr. Nabeela Kausar (External Examiner) Dr. Ambreen Afsar Khan (Internal Examiner)

3._____________________ 4. ____________________

Dr. Khadija Maqbool (Supervisor) Prof. Dr. Nasir Ali (Chairman)

Department of Mathematics & Statistics
Faculty of Sciences
International Islamic University, Islamabad
Pakistan

2024

Thesis Certificate

The thesis entitled ***"Heat Transfer Analysis of Viscoelastic Fluid Flow in a Peripheral Layer"*** submitted by ***Mehwish***, ***833-FBAS/MSMA/F22*** in partial fulfillment of MS Degree in Mathematics has been completed under my guidance and supervision. I am satisfied with the quality of her research work and allow her to submit this thesis for further process to graduate with Master of Science degree from the Department of Mathematics & Statistics, as per IIUI rules and regulations.

Date…………………………. ____________________

Dr. Khadija Maqbool
Assistant Professor
Department of Maths & Stats
International Islamic University,
Islamabad.

DECLARATION

I hereby declare that this thesis, neither as a whole nor a part of it, has been copied out from any source. It is further declared that I have prepared this dissertation entirely based on my efforts under the supervision of my supervisor **Dr. Khadija Maqbool**. No portion of the work, presented in this dissertation, has been submitted in the support of any application for any degree or qualification of this or any other learning institute.

Mehwish
MS (Mathematics)
Reg. No. 833-FBAS/MSMA/F22
Department of Mathematics and Statistics
Faculty of Sciences,
International Islamic University Islamabad, Pakistan.

Dedication

First of all, I dedicate this thesis to Allah Almighty and the Holy Prophet (P.B.U.H). Secondly, I dedicate this thesis to my respected parents who pray for me all the time. I also dedicate it to my teachers who guided me at every stage, and then to all my family members, who helped and encouraged me.

Acknowledgments

All praise and glory to **Allah Almighty** Who gave me the strength and courage to understand, learn, and complete this thesis.

I would like to express my sincere gratitude to my supervisor, my mentor, **Dr. Khadija Maqbool**, for her continuous support and guidance. Her patience, motivation, enthusiasm, and immense knowledge have been invaluable throughout my research work. She voluntarily gave me precious time whenever I needed it.

I would also like to thank my dear parents, **Mr. and Mrs. Hafiz Ahmed Yar**, and my brothers, **Shaheryar Ahmed, Abrar Ahmed** and my sister, **Sehrish Ahmed**, who have always supported me. Without their unwavering support, I would not have reached the pinnacle of success. They kept me motivated and understanding, and their encouragement and guidance since my childhood have enabled me to unfold my hidden abilities.

Sincere thanks to all my friends for their kindness and moral support during my study. Thanks for the friendship and memories.

Lastly, I offer my regards and blessings to all of those who supported me in any aspect during the completion of this thesis.

(Mehwish)

Contents

Preface

Ciliary flow has been a subject of scientific study from few decades because of its applications in physiological and bioengineering science. Cilia has a structure like hair and its movement is rhythmic and follow the wavy pattern which is formed by effective and recovery stroke. Ciliary movement and its frequency is effected by the surrounding temperature, therefore a number of researchers investigated the effect of heat transfer on ciliary flow of Newtonian and non-Newtonian fluids.

Maqbool et. al. [1] investigated the magnetohydrodynamic convective flow of Carreau fluid through a ciliated channel. Sadaf et. al. [2] presented the MHD convective flow through a curved channel anchored with cilia. Akbar et. al. [3] investigated the physical aspects of electro osmosis and thermal radiation of couple stress fluid through a symmetric and asymmetric ciliated channel. She further studied the MHD and heat transfer effect on flow due to metachronal wave of cilia and found the exact solution for pressure and velocity in Ref. [4]. Further Imran et. al. [5] modeled the convective flow of Williamson fluid under electro osmotic effect and found the analytical solution for velocity, pressure, temperature and stream functions using the perturbation technique. Bhatti et. al. [6], Mills et. al. [7], Butt. et. al. [8], Rafiq et. al. [9] and Akbar et. al. [10] proposed ciliary flow of different fluid models in different geometry using thermal effect.

In ciliary flows, two immiscible fluid have vital role, therefore few studies on two layered ciliary flow have been presented. Rajashekhar et. al. [11], Ashraf et. al. [12], Fatima et. al. [13] and Asghar et. al. [14] considered the Harschel Bukley model, Jeffrey fluid model, Newtonian fluid and Ellis fluid to discuss the two layer flow due to wavy boundary The study of Ellis fluid due to peristaltic movement under the magnetic, thermal and osmotic effect have presented by different researchers in Refs. [15-21], but two layer ciliary flow of Ellis fluid under the buoyancy effect has not been discussed earlier.

The present thesis analyze the viscoelastic fluid flow in two layer ciliary flow and is organized in following three chapters. Chapter one deals with the basic laws of fluid mechanics and basic definitions. Chapter two includes the two phase flow of Newtonian fluid through a ciliated channel and chapter three presents the viscoelastic Ellis fluid flow in a ciliated channel under thermal and buoyancy effect.

Chapter 1

Introduction

The definitions regarding this research are provided in this chapter.

1.1 Fluid

Fluid is a substance that can not have a particular shape, it deforms under the action of applied shear stress. Liquids, solids and polymers are categorized as fluids.

1.2 Fluid Mechanics

It is the study of fluids subject to the given constraints, fluid mechanics deals with the movement of the fluid particles and fluid at rest. Fluid dynamics is divided into three disciplines, analytical fluid mechanics, numerical fluid mechanics and experimental fluid mechanics.

1.3 Multiphase Flow

Multiphase flow consists of more than one phase or components which has separation at a smaller scale but above the molecular level. Multiphase flow can be classified as disperse flows (e.g. drops or bubbles) and separated flows.

1.3.1 Types of Multiphase Flow

The most common class of Multiphase flow are two phase flows and these include

1) Gas-liquid flow
2) Gas-solid flow
3) Liquid-liquid flow
4) Liquid-solid flow

1.4 Properties of Flow

There are important fluid properties other than velocity and temperature, which are described as follows

1.4.1 Viscosity

Viscosity is the property of the fluid which offers resistance to the movement of one layer of the fluid over another adjacent layer of the fluid because of shear stress. Mathematically,

$$\mu = \frac{\tau_{yx}}{\frac{du}{dx}}, \tag{1.1}$$

where $\frac{du}{dx}$ is velocity gradient and τ_{yx} is shear stress.

1.4.2 Pressure

Pressure is defined as the magnitude of the force applied perpendicular to the surface area of an object. Symbolically, it can be expressed as

$$P = \frac{|F|}{A}. \tag{1.2}$$

1.4.3 Shear Stress

It expresses the efforts of a force parallel to the surface of interest. Mathematically, it is defined as

$$\tau = \frac{F}{A}, \tag{1.3}$$

where F is the force parallel to the surface and A is the surface area.

1.5 Classification of Fluid

1.5.1 Newtonian and Non-Newtonian Fluid

The fluid which follows Newton's law of viscosity is defined as Newtonian fluid whereas fluid that does not exhibit the property of constant viscosity and effected by shear stress is categorized as a non-Newtonian fluid.

1.6 Dimensionless Numbers

There are different non dimensional quantities that appear in non dimensional, incompressible, momentum and energy equation and are described as follows:

1.6.1 Reynold's Number

It quantifies the influence of viscosity over the acceleration field. It does this by comparing the magnitude of inertial effects to viscous effect. Mathematically,it is defined as:

$$\mathrm{Re} = \frac{\rho v L}{\mu}, \tag{1.4}$$

where L is the length, v is the speed of wave, ρ is the density and μ is the dynamic viscosity.

1.6.2 Prandtl Number

It relates the relation between kinematic viscosity of the fluid and diffusive property of the fluid due to heat. Mathematically,

$$\mathrm{Pr} = \frac{\mu C_p}{k}, \tag{1.5}$$

where ν is the thermal conductivity, μ is the dynamic viscosity and C_p is specific heat due to pressure.

1.6.3 Grashof Number

Grashof number is a dimensionless number which approximates the ratio of buoyancy to viscous forces acting on a fluid. Mathematically,

$$Gr = \frac{ga^3\beta(T_1 - T_0)}{\nu^2}, \tag{1.6}$$

where g is gravitational acceleration , β is the coefficient of volume expansion, T_1 is the surface temperature, T_0 is the bulk temperature, a is the surface length, and ν is the kinematic viscosity.

1.7 Heat Transfer

Heat transmission takes place when there is a difference in temperature amongst the boundary and fluid. It is classified into different mechanisms e.g., conduction, convection and radiation.

1.7.1 Conduction

Conduction takes place when heat energy is transferred through collisions between neighboring atoms or molecules. In solids and liquids, heat is transmitted through conduction due to less distance between particles.

1.7.2 Convection

Convection occurs when there is a bulk movement of molecules, this mode of heat transfer takes place in case of liquids and gases. Further, it can be classified into following types:

Natural Convection

Natural convection occurs due to the buoyancy force which appears due to density difference in the presense of temperature difference, e.g. oceanic winds give rise to natural convection.

Forced Convection

Convection induced by some external sources such as fans and pumps is known as forced convection, e.g. geysers or water heaters and fans used in summer.

Mixed Convection

Mixed convection includes both natural and forced convection.

1.7.3 Radiation

Radiation is the mode of heat transfer which does not require any medium to propagate, and energy is transferred from hot object to cold object either in the form of electromagnetic waves or photons.

1.8 Ciliary Surface

Most of the biological fluid flows are due to small hair like structures called Cilia, present on surface of various organs. A single cilium is usually of length 1-10 micrometers, and are categorized into motile and non motile cilia. Motile cilia helps for the locomotion of the fluid in a body while non motile cilia helps to pass the signals in sensory organs.

1.8.1 Metachronal Waves

Ciliary tip follows elliptical path that give rise to wavy motion and appears like travelling waves called metachronal waves.

1.9 Basic Laws of Fluid Mechanics

1.9.1 Principle of Conservation of Mass

This law states that mass can neither be created nor destroyed and remains constant for a system. Mathematically, for two phase flow it is stated as follows:

$$\frac{\partial p^{(k)}}{\partial t} + \mathbf{\nabla}.(\rho^{(k)}\mathbf{V}^{(k)}) = 0, \tag{1.7}$$

where $\rho^{(k)}$ is the fluid density, t is the time, $\mathbf{\nabla}$ represents divergence and $\mathbf{V}^{(k)}$ is the velocity vector. The superscript $(k = 1, 2)$ refers to the fluid in layer I and layer II. For incompressible flow, density of fluid is constant so the equation (1.7) takes the following form:

$$\boldsymbol{\nabla}.\mathbf{V}^{(k)} = 0. \tag{1.8}$$

1.9.2 Principle of Conservation of Momentum

It is law of motion which states that net momentum of an isolated system remains conserved within the system unless an external force is applied. For two phase fluid flow, this law can be expressed as follows

$$\rho^{(k)}\frac{d\mathbf{V}^{(k)}}{dt} - \boldsymbol{\nabla}.\boldsymbol{\tau}^{(k)} = \rho\mathbf{b}, \tag{1.9}$$

where $\frac{d}{dt}$ is the total derivative, $\boldsymbol{\tau}^{(k)}$ shows the Cauchy stress tensor, $\mathbf{b}$ is the body force and $\rho^{(k)}$ shows the density of fluid in both layers.

In rectangular coordinates system equation (1.9) can be expressed as follows

$$\rho^{(k)}\left(\frac{\partial u^{(k)}}{\partial t} + u^{(k)}\frac{\partial u^{(k)}}{\partial x} + v^{(k)}\frac{\partial u^{(k)}}{\partial y} + w^{(k)}\frac{\partial u^{(k)}}{\partial z}\right) = \frac{\partial \tau_{xx}^{(k)}}{\partial x} + \frac{\partial \tau_{xy}^{(k)}}{\partial y} + \frac{\partial \tau_{xz}^{(k)}}{\partial z} + \rho^{(k)}b_x, \tag{1.10}$$

$$\rho^{(k)}\left(\frac{\partial v^{(k)}}{\partial t} + u^{(k)}\frac{\partial v^{(k)}}{\partial x} + v^{(k)}\frac{\partial v^{(k)}}{\partial y} + w^{(k)}\frac{\partial v^{(k)}}{\partial z}\right) = \frac{\partial \tau_{yx}^{(k)}}{\partial x} + \frac{\partial \tau_{yy}^{(k)}}{\partial y} + \frac{\partial \tau_{yz}^{(k)}}{\partial z} + \rho^{(k)}b_y, \tag{1.11}$$

$$\rho^{(k)}\left(\frac{\partial w^{(k)}}{\partial t} + u^{(k)}\frac{\partial w^{(k)}}{\partial x} + v^{(k)}\frac{\partial w^{(k)}}{\partial y} + w^{(k)}\frac{\partial w^{(k)}}{\partial z}\right) = \frac{\partial \tau_{zx}^{(k)}}{\partial x} + \frac{\partial \tau_{zy}^{(k)}}{\partial y} + \frac{\partial \tau_{zz}^{(k)}}{\partial z} + \rho^{(k)}b_z. \tag{1.12}$$

1.9.3 Principle of Conservation of Energy

This law states that energy can neither be created nor destroyed. Mathematically, it can be written as follows

$$\rho^{(k)}c_p^{(k)}\frac{dT^{(k)}}{dt} = K^{(k)}\boldsymbol{\nabla}^2T^{(k)} + Q_0, \tag{1.13}$$

where $c_p^{(k)}$ is specific heat of fluid, $T^{(k)}$ is temperature in both layers and Q_0 is heat source.

Chapter 2

Heat Transfer Analysis of Two Phase Flow in a Ciliated Surface

This chapter deals with heat transfer analysis of immiscible flow of Newtonian fluid due to ciliary movements through a channel. Convective flow in the presence of buoyancy force and heat source is considered and analytical results for flow has been presented. Mathematical model of the problem represents the complex system of partial differential equations which are simplified by the lubrication approach. Exact solutions for velocity profile, temperature profile, pressure gradient and volume flow rate are calculated and influence of different flow parameters appearing in the study is explained graphically.

2.1 Formulation of the Problem

Newtonian fluid flow is assumed to be unsteady and incompressible through a ciliated channel. Wavy movement is formed by the collective beating of cilia that generates the metachronal waves in (X^*, Y^*) coordinate system and tips of cilia follow an elliptical path described by the following parametric equations:

$$X^* = f(X^*, X_0^*, t^*) = X_0^* + a\epsilon\alpha \sin\left(2\pi\left(\frac{X^* - ct^*}{\lambda}\right)\right), \tag{2.1}$$

$$Y^* = f''(X^*, t^*) = a + a\epsilon \cos\left(2\pi\left(\frac{X^* - ct^*}{\lambda}\right)\right), \tag{2.2}$$

where ϵ is a non dimensional parameter w.r.t cilia length, $X_0^*$is the reference position of cilia, α is the eccentricity of ellipse, λ and c are the wavelength and wave speed of metachronal wave respectively.

The velocity profile of the problem is given by

$$V^{*(k)} = \left[U^{*(k)}(X^*, Y^*, t^*), V^{*(k)}(X^*, Y^*, t^*), 0\right], \tag{2.3}$$

where $U^{*(k)}$ and $V^{*(k)}$ are the components of velocity in horizontal and vertical directions respectively. Superscripts k corresponds to fluid in two layers.

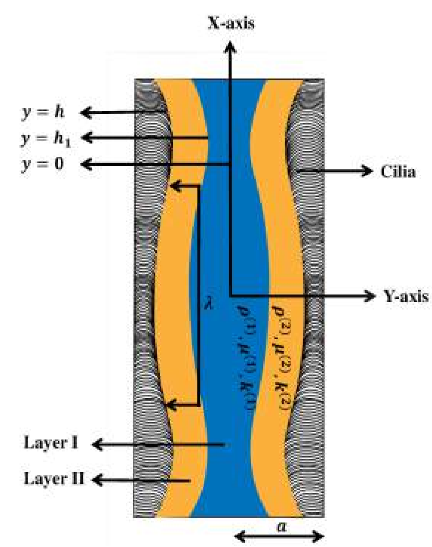

Fig. 2.1: Geometry of the flow problem

Governing equations of mathematical model are formulated by continuity, momentum and energy equation.

$$\boldsymbol{\nabla}.\mathbf{V}^{*(k)} = 0, \tag{2.4}$$

$$\rho^{*(k)}\frac{d\mathbf{V}^{*(k)}}{dt^*} = \text{div}\,\boldsymbol{\tau}^{(k)} + \rho^{*(k)}\mathbf{b}, \tag{2.5}$$

$$\rho^{*(k)}c_p^{(k)}\frac{dT^{*(k)}}{dt^*} = K^{(k)}\boldsymbol{\nabla}^2 T^{(k)} + Q_0, \tag{2.6}$$

where $\rho^{*(k)}$ denotes density, $\tau^{(k)}$ is stress tensor for Newtonian fluid and is given by

$$\boldsymbol{\tau}^{(k)} = -P^* I + \mu^{(k)} A_1, \tag{2.7}$$

$$A_1 = \boldsymbol{\nabla}\mathbf{V}^{*(k)} + \left(\boldsymbol{\nabla}\mathbf{V}^{*(k)}\right)^t, \tag{2.8}$$

$P^*$is the pressure, I represents identity matrix, A_1 is the first Rivilian Erickson tensor, $c_p^{(k)}$ gives specific heat at constant pressure, $K^{(k)}$ is thermal conductivity and Q_0 reflects heat source term.

No slip condition suggests that the fluid particles lying adjacent to cilia tips will have same velocity as that of cilia tips and are given as follows:

$$U^{*(k)} = \frac{\partial f}{\partial t^*} + \frac{\partial f}{\partial X^*}\frac{\partial X^*}{\partial t^*} = \frac{\partial f}{\partial t^*} + \frac{\partial f}{\partial X^*}U^*, \tag{2.9}$$

$$V^{*(k)} = \frac{\partial f''}{\partial t^*} + \frac{\partial f''}{\partial X^*}\frac{\partial X^*}{\partial t^*} = \frac{\partial f''}{\partial t^*} + \frac{\partial f''}{\partial X^*}U^*. \tag{2.10}$$

Using Eqs. (2.1)-(2.2) in Eqs. (2.9)-(2.10) one can get following form of velocity at the boundary.

$$U^* = \frac{-\frac{2\pi}{\lambda}\epsilon\alpha ac\cos\left(2\pi\left(\frac{X^*-ct^*}{\lambda}\right)\right)}{1-\frac{2\pi}{\lambda}\epsilon\alpha ca\cos\left(2\pi\left(\frac{X^*-ct^*}{\lambda}\right)\right)}, \tag{2.11}$$

$$V^* = \frac{\frac{2\pi}{\lambda}\epsilon ac\sin\left(2\pi\left(\frac{X^*-ct^*}{\lambda}\right)\right)}{1-\frac{2\pi}{\lambda}\epsilon\alpha a\cos\left(2\pi\left(\frac{X^*-ct^*}{\lambda}\right)\right)}, \tag{2.12}$$

where U^* and V^* are boundary conditions at

$$Y^* = \pm a\left(1+\epsilon\cos\left(2\pi\left(\frac{X^*-ct^*}{\lambda}\right)\right)\right). \tag{2.13}$$

The ciliary flow from fixed to wave frame is transformed under the following transformations:

$$p^*(x^*,y^*) = P^*(X^*,Y^*,t^*), y^* = Y^*, x^* = X^*-ct^*, v^* = V^*, u^* = U^*-c. \tag{2.14}$$

Using above relations Eqs.(2.4-2.6) in fixed frame take the following form: $\frac{\partial u^{*(k)}}{\partial x^*} + \frac{\partial v^{*(k)}}{\partial y^*} = 0,$

$$\rho^{*(k)}\left(\left(u^{*(k)}+c\right)\frac{\partial u^{*(k)}}{\partial x^*} + v^{*(k)}\frac{\partial u^{*(k)}}{\partial y^*}\right) = -\frac{\partial p^*}{\partial x^*} + \frac{\partial \tau_{xx}^{*(k)}}{\partial x^*} + \frac{\partial \tau_{xy}^{*(k)}}{\partial y^*} + \rho^{(k)} g\beta(T^*-T_0^*), \tag{2.15}$$

$$\rho^{*(k)}\left(\left(u^{*(k)}+c\right)\frac{\partial v^{*(k)}}{\partial x^*}+v^{*(k)}\frac{\partial v^{*(k)}}{\partial y^*}\right)=-\frac{\partial p^*}{\partial y^*}+\frac{\partial \tau_{yx}^{*(k)}}{\partial x^*}+\frac{\partial \tau_{yy}^{*(k)}}{\partial y^*}, \tag{2.16}$$

$$\rho^{*(k)}c_p^{(k)}\left(\left(u^{*(k)}+c\right)\frac{\partial T^{*(k)}}{\partial x^*}+v^{*(k)}\frac{\partial T^{*(k)}}{\partial y^*}\right)=K^{(k)}\left(\frac{\partial^2 T^{*(k)}}{\partial x^{*2}}+\frac{\partial^2 T^{*(k)}}{\partial y^{*2}}\right)+Q_0, \tag{2.17}$$

$$\tau_{xy}^{*(k)}=\mu^{*(k)}\left(\frac{\partial v^{*(k)}}{\partial x^*}+\frac{\partial u^{*(k)}}{\partial y^*}\right), \tag{2.18}$$

$$\tau_{xx}^{*(k)}=2\mu^{*(k)}\frac{\partial u^{*(k)}}{\partial x^*}, \tag{2.19}$$

$$\tau_{yy}^{*(k)}=2\mu^{*(k)}\frac{\partial v^{*(k)}}{\partial y^*}. \tag{2.20}$$

Since biological flows are Poiseuille type, therefore flow and temperature are assumed to be maximum at center line $y=0$ therefore, boundary conditions take the following form

$$\tau_{xy}^{*(1)}=0, \text{ at } y^*=0, \tag{2.21}$$

$$\tau_{xy}^{*(1)}=\tau_{xy}^{*(2)}, \text{ at } y^*=h_1^*, \tag{2.22}$$

$$u^{*(1)}=u^{*(2)}, \text{ at } y^*=h_1^*, \tag{2.23}$$

$$u^{*(2)}+c=\frac{-\frac{2\pi}{\lambda}\epsilon\alpha ac\cos\left(\frac{2\pi x^*}{\lambda}\right)}{1-\frac{2\pi}{\lambda}\epsilon\alpha ac\cos\left(\frac{2\pi x^*}{\lambda}\right)}, \text{ at } y^*=h^*, \tag{2.24}$$

$$v^{*(2)}=\frac{\frac{2\pi}{\lambda}\epsilon ac\sin\left(\frac{2\pi x^*}{\lambda}\right)}{1-\frac{2\pi}{\lambda}\epsilon\alpha a\cos\left(\frac{2\pi x^*}{\lambda}\right)}, \text{ at } y^*=h^*. \tag{2.25}$$

Temperature profile at boundary is given by

$$\frac{\partial T^{*(k)}}{\partial y^*}=0, \text{ at } y^*=0, \tag{2.26}$$

$$K^{(1)}\frac{\partial T^{*(1)}}{\partial y^*}=K^{(2)}\frac{\partial T^{*(2)}}{\partial y^*}, \text{ at } y^*=h_1^*, \tag{2.27}$$

$$T^{*(1)}=T^{*(2)}, \text{ at } y^*=h_1^*, \tag{2.28}$$

$$T^{*(2)}=T_1, \text{ at } y^*=h^*, \tag{2.29}$$

where

$$h^* = \pm \left(a + a\epsilon \cos\left(\frac{2\pi x^*}{\lambda}\right)\right), \tag{2.30}$$

$$h_1^* = \pm \left(a + a\epsilon \cos\left(\frac{2\pi x^*}{\lambda}\right)\right). \tag{2.31}$$

Non dimensional parameters are introduced as follows

$$\begin{aligned}
x &= \frac{x^*}{\lambda},\ y = \frac{y^*}{a},\ u^{(k)} = \frac{u^{*(k)}}{c},\ v^{(k)} = \frac{v^{*(k)}}{\gamma c},\ h = \frac{h^*}{a},\ h_1 = \frac{h_1^*}{a},\ p = \frac{a\gamma}{c\mu^{(1)}}p^*,\\
\gamma &= \frac{a}{\lambda},\ \mathrm{Re} = \frac{\rho a c}{\mu^{(1)}},\ \mathrm{Pr} = \frac{\mu^{(1)}c_p}{k^{(k)}},\ \theta = \frac{T^{*(k)} - T_0^*}{T_1^* - T_0^*},\ \rho^{(k)} = \frac{\rho^{*(k)}}{\rho^{(1)}},\ \mu^{(k)} = \frac{\mu^{*(k)}}{\mu^{(1)}},\\
k^{(k)} &= \frac{k^{*(k)}}{k^{(1)}},\ Gr = \frac{ga^3\beta(T_1^* - T_0^*)}{\nu^2},\ b = \frac{a^2 Q_0}{(T_1^* - T_0^*)\mu^{(1)}c_p},\ \delta = \frac{a_1}{a},\ Gr_t = \frac{Gr}{\mathrm{Re}},\\
\tau_{ij}^{(k)} &= \frac{a}{c\mu^{(1)}}\tau_{ij}^{*(k)}.
\end{aligned} \tag{2.32}$$

Using above parameters Eqs. (2.15)-(2.32) reduce into the following form

$$\frac{\partial u^{(k)}}{\partial x} + \frac{\partial v^{(k)}}{\partial y} = 0, \tag{2.33}$$

$$\mathrm{Re}\,\gamma\left(\left(u^{(k)}+1\right)\frac{\partial u^{(k)}}{\partial x} + v^{(k)}\frac{\partial u^{(k)}}{\partial y}\right) = -\frac{\partial p}{\partial x} + \gamma\frac{\partial \tau_{xx}^{(k)}}{\partial x} + \frac{\partial \tau_{xy}^{(k)}}{\partial y} + Gr_t\theta^{(k)}, \tag{2.34}$$

$$\mathrm{Re}\,\gamma^3\left(\left(u^{(k)}+1\right)\frac{\partial v^{(k)}}{\partial x} + v^{(k)}\frac{\partial v^{(k)}}{\partial y}\right) = -\frac{\partial p}{\partial y} + \gamma^2\frac{\partial \tau_{yx}^{(k)}}{\partial x} + \gamma\frac{\partial \tau_{yy}^{(k)}}{\partial y}, \tag{2.35}$$

$$\mathrm{Pr}\,\mathrm{Re}\,\gamma\left(\left(u^{(k)}+1\right)\frac{\partial \theta^{(k)}}{\partial x} + v^{(k)}\frac{\partial \theta^{(k)}}{\partial y}\right) = \gamma^2\left(\frac{\partial^2 \theta^{(k)}}{\partial x^2} + \frac{\partial^2 \theta^{(k)}}{\partial y^2}\right) + \mathrm{Pr}\,b, \tag{2.36}$$

$$\tau_{xy}^{(k)} = \mu^{(k)}\left(\gamma^2\frac{\partial v^{(k)}}{\partial x} + \frac{\partial u^{(k)}}{\partial y}\right), \tag{2.37}$$

$$\tau_{xx}^{(k)} = 2\gamma\mu^{(k)}\frac{\partial u^{(k)}}{\partial x}, \tag{2.38}$$

$$\tau_{yy}^{(k)} = 2\gamma\mu^{(k)}\frac{\partial v^{(k)}}{\partial y}, \tag{2.39}$$

with boundary conditions

$$\tau_{xy}^{(1)} = 0,\ \text{at } y = 0, \tag{2.40}$$

$$\tau_{xy}^{(1)} = \tau_{xy}^{(2)}, \text{ at } y = h_1, \tag{2.41}$$

$$u^{(1)} = u^{(2)}, \text{ at } y = h_1, \tag{2.42}$$

$$u^{(2)} = \frac{-2\pi\epsilon\alpha\gamma\cos(2\pi x)}{1 - 2\pi\epsilon\alpha\gamma\cos(2\pi x)} - 1, \text{ at } y = h, \tag{2.43}$$

$$v^{(2)} = \frac{2\pi\epsilon\gamma c\sin(2\pi x)}{1 - 2\pi\epsilon\alpha\gamma\cos(2\pi x)}, \text{ at } y = h. \tag{2.44}$$

Temperature profile at boundary is given by

$$\frac{\partial\theta^{(1)}}{\partial y} = 0, \text{ at } y = 0, \tag{2.45}$$

$$K^{(1)}\frac{\partial\theta^{(1)}}{\partial y} = K^{(2)}\frac{\partial\theta^{(2)}}{\partial y}, \text{ at } y = h_1, \tag{2.46}$$

$$\theta^{(1)} = \theta^{(2)}, \text{ at } y = h_1, \tag{2.47}$$

$$\theta^{(2)} = 1, at\ y = h, \tag{2.48}$$

where

$$h = \pm\left(1 + \epsilon\cos(2\pi x)\right), \tag{2.49}$$

$$h_1 = \pm\delta\left(1 + \epsilon\cos(2\pi x)\right). \tag{2.50}$$

For the slow biological flow, small Reynold's number and wavelength assumption reduces the Eqs. (2.35-2.45) into the following form:

$$-\frac{\partial p}{\partial x} + \frac{\partial\tau_{xy}^{(k)}}{\partial y} + Gr_t\theta^{(k)} = 0, \tag{2.51}$$

$$-\frac{\partial p}{\partial y} = 0, \tag{2.52}$$

$$\frac{\partial^2\theta^{(k)}}{\partial y^2} + \Pr b = 0, \tag{2.53}$$

$$\tau_{xy}^{(k)} = \mu^{(k)}\frac{\partial u^{(k)}}{\partial y}, \tag{2.54}$$

$$\tau_{xx}^{(k)} = 0, \tag{2.55}$$

$$\tau_{yy}^{(k)} = 0, \tag{2.56}$$

with boundary conditions

$$\tau_{xy}^{(1)} = 0, \text{ at } y = 0, \tag{2.57}$$

$$\tau_{xy}^{(1)} = \tau_{xy}^{(2)}, \text{ at } y = h_1, \tag{2.58}$$

$$u^{(1)} = u^{(2)}, \text{ at } y = h_1, \tag{2.59}$$

$$u^{(2)} = -2\pi\epsilon\alpha\gamma\cos(2\pi x) - 1, \text{ at } y = h, \tag{2.60}$$

$$v^{(2)} = 2\pi\epsilon\gamma\sin(2\pi x) + (2\pi\epsilon\gamma)^2\alpha\sin(2\pi x)\cos(2\pi x), \text{ at } y = h. \tag{2.61}$$

Temperature profile at boundary is given by

$$\frac{\partial\theta^{(1)}}{\partial y} = 0, \text{ at } y = 0, \tag{2.62}$$

$$K^{(1)}\frac{\partial\theta^{(1)}}{\partial y} = K^{(2)}\frac{\partial\theta^{(2)}}{\partial y}, \text{ at } y = h_1, \tag{2.63}$$

$$\theta^{(1)} = \theta^{(2)}, \text{ at } y = h_1, \tag{2.64}$$

$$\theta^{(2)} = 1, \text{ at } y = h. \tag{2.65}$$

2.2 Solution of the Problem

Upon integration of Eq. (2.54) one can get following form of temperature profile:

$$\theta^{(k)} = -\frac{\Pr by^2}{2} + A^{(k)}y + B^{(k)}, \tag{2.66}$$

where $A^{(k)}$ and $B^{(k)}$ are constants of integration and are determined by the boundary conditions given in Eqs. (2.63)-(2.66)

$$A^{(1)} = 0, \; 0 \le y \le h_1, \tag{2.67}$$

$$B^{(1)} = 1 + \Pr b\left(\left(1 - \frac{k^{(1)}}{k^{(2)}}\right)h_1(h_1 - h) + \frac{h^2}{2}\right), \; 0 \le y \le h_1, \tag{2.68}$$

$$A^{(2)} = \left(1 - \frac{k^{(1)}}{k^{(2)}}\right) \Pr b h_1, \;\; h_1 \leq y \leq h, \tag{2.69}$$

$$B^{(2)} = 1 + \Pr b h \left(\frac{h}{2} - h_1 \left(1 - \frac{k^{(1)}}{k^{(2)}}\right)\right) \;\; h_1 \leq y \leq h. \tag{2.70}$$

Using Eqs. (2.68-2.71) in Eq. (2.67) one can get the temperature profiles for two regions which are given as follows

$$\theta^{(1)} = 1 - \Pr b \left(\frac{\left(y^2 - h^2\right)}{2} - \left(1 - \frac{k^{(1)}}{k^{(2)}}\right) h_1 \left(h_1 - h\right)\right), \tag{2.71}$$

$$\theta^{(2)} = 1 - \Pr b \left(\frac{\left(y^2 - h^2\right)}{2} - \left(1 - \frac{k^{(1)}}{k^{(2)}}\right) h_1 \left(y - h\right)\right). \tag{2.72}$$

Rewrite Eq. (2.52) for two regions in terms of temperature profiles

$$\frac{\partial p}{\partial x} = \frac{\partial \tau_{xy}^{(1)}}{\partial y} + Gr_t \left(1 - \Pr b \left(\frac{\left(y^2 - h^2\right)}{2} - \left(1 - \frac{k^{(1)}}{k^{(2)}}\right) h_1 \left(h_1 - h\right)\right)\right), \tag{2.73}$$

$$\frac{\partial p}{\partial x} = \frac{\partial \tau_{xy}^{(2)}}{\partial y} + Gr_t \left(1 - \Pr b \left(\frac{\left(y^2 - h^2\right)}{2} - \left(1 - \frac{k^{(1)}}{k^{(2)}}\right) h_1 \left(y - h\right)\right)\right). \tag{2.74}$$

It is evident from Eq. (2.53), that pressure is a function of x only.

$$p \neq p(y). \tag{2.75}$$

Integrating Eqs. (2.74-2.75) w.r.t y and using boundary conditions (2.58-2.59) one can get following form of shear stress:

$$\tau_{xy}^{(1)} = \frac{dp}{dx} y - Gr_t \left(\Pr b y \left(-\frac{y^2}{6} + \left(1 - \frac{k^{(1)}}{k^{(2)}}\right)\left(h_1^2 - h_1 h\right) + \frac{h^2}{2}\right) + y\right) \;\; 0 \leq y \leq h_1 \tag{2.76}$$

$$\tau_{xy}^{(2)} = \frac{dp}{dx} y - Gr_t \left(\Pr b y \left(-\frac{y^2}{6} + \left(\frac{h^2}{2} - h_1 \left(1 - \frac{k^{(1)}}{k^{(2)}}\right)\left(h - \frac{y}{2}\right)\right)\right) + y\right), \;\; h_1 \leq y \leq h. \tag{2.77}$$

Integrating Eqs. (2.77-2.78) w.r.t y and applying boundary conditions given in (2.60-2.61) one can get following velocity profile for both regions

$$\begin{aligned} u^{(1)} &= \frac{1}{2}\left(\frac{dp}{dx}\right)\left(\frac{\left(y^2-h_1^2\right)}{\mu^{(1)}}+\frac{\left(h_1^2-h^2\right)}{\mu^{(2)}}\right)+u(h) \\ &+\frac{Gr_t}{2}\left(\begin{array}{c} \frac{\Pr b}{12}\left(\frac{\left(y^4-h_1^4\right)}{\mu^{(1)}}+\frac{\left(h_1^4-h^4\right)}{\mu^{(2)}}\right)+ \\ \frac{B^{(1)}\left(h_1^2-y^2\right)}{\mu^{(1)}}-\frac{B^{(2)}\left(h_1^2-h^2\right)}{\mu^{(2)}}-\frac{A^{(2)}\left(h_1^3-h^3\right)}{3\mu^{(2)}} \\ -\frac{2h_1}{\mu^{(2)}}\left(B^{(1)}-B^{(2)}\right)(h_1-h)+\frac{h_1^2}{\mu^{(2)}}A^{(2)}(y-h) \end{array}\right), \end{aligned} \tag{2.78}$$

$$\begin{aligned} u^{(2)} &= \frac{1}{2\mu^{(2)}}\left(\frac{dp}{dx}\right)\left(y^2-h^2\right)+u(h)+ \\ &\frac{Gr_t}{6}\left(\begin{array}{c} \frac{\Pr b\left(y^4-h^4\right)}{4\mu^{(2)}}-\frac{A^{(2)}\left(y^3-h^3\right)}{\mu^{(2)}}-\frac{3B^{(2)}\left(y^2-h^2\right)}{\mu^{(2)}} \\ -\frac{6h_1}{\mu^{(2)}}\left(B^{(1)}-B^{(2)}\right)(y-h)+\frac{3h_1^2}{\mu^{(2)}}A^{(2)}(y-h) \end{array}\right). \end{aligned} \tag{2.79}$$

To find the expression of vertical velocity, Eq. (2.34) in the following form is used:

$$\frac{\partial v^{(k)}}{\partial y} = -\frac{\partial u^{(k)}}{\partial x}. \tag{2.80}$$

Integrating Eq. (2.81), solving for $v^{(k)}$and using no slip boundary condition, one can get the following speed in transverse direction:

$$v^{(1)} = -\frac{1}{2}\left(\frac{d^2p}{dx^2}\right)\left(\begin{array}{c} \frac{\left(\frac{y^3}{3}-yh_1^2\right)}{\mu^{(1)}}+\frac{\left(h_1^2-h^2\right)y}{\mu^{(2)}} \\ +\frac{2\left(h^3-h_1^3\right)}{3\mu^{(2)}}+\frac{2h_1^3}{3\mu^{(1)}} \end{array}\right)+v(h)-(y-h)\frac{\partial u(h)}{\partial x}, \tag{2.81}$$

$$v^{(2)} = -\frac{1}{6\mu^{(2)}}\left(\frac{d^2p}{dx^2}\right)\left(3\left(\frac{y^3}{3}-yh^2\right)+2h^3\right)+v(h)-(y-h)\frac{\partial u(h)}{\partial x}. \tag{2.82}$$

To observe the flow patterns, following relation of stream function is used:

$$\frac{\partial \psi^{(k)}}{\partial y} = u^{(k)}, \tag{2.83}$$

$$\frac{\partial \psi^{(k)}}{\partial x} = -v^{(k)}. \tag{2.84}$$

Using Eqs. (2.84-2.85), one can get expressions for stream functions for layer I and II,

$$\begin{aligned}\psi^{(1)} &= \left(\frac{dp}{dx}\right)\left(\frac{\left(\frac{y^3}{3}-yh_1^2\right)}{2\mu^{(1)}}+\frac{\left(h_1^2-h^2\right)y}{2\mu^{(2)}}-\frac{\left(h_1^3-h^3\right)}{3\mu^{(2)}}+\frac{h_1^3}{3\mu^{(1)}}\right)\\ &-\int v(h)dx+(y-h)u(h)+\\ &Gr_t\left(\begin{array}{c}\frac{\Pr b}{24}\left(\frac{\left(\frac{y^5}{5}-yh_1^4\right)}{\mu^{(1)}}+\frac{\left(h_1^4-h^4\right)y}{\mu^{(2)}}\right)\\ +\frac{B^{(1)}\left(yh_1^2-\frac{y^3}{3}\right)}{2\mu^{(1)}}-\frac{B^{(2)}\left(h_1^2-h^2\right)y}{2\mu^{(2)}}-\frac{A^{(2)}\left(h_1^3-h^3\right)y}{6\mu^{(2)}}\\ -\frac{yh_1}{\mu^{(2)}}\left(B^{(1)}-B^{(2)}\right)(h_1-h)+\frac{h_1^2y}{2\mu^{(2)}}A^{(2)}(h_1-h)\end{array}\right),\end{aligned} \tag{2.85}$$

$$\begin{aligned}\psi^{(2)} &= \frac{1}{2\mu^{(2)}}\left(\frac{dp}{dx}\right)\left(\frac{y^3}{3}-yh^2+\frac{2h^3}{3}\right)-\int v(h)dx+(y-h)u(h)+\\ &Gr_t\left(\begin{array}{c}\frac{\Pr b}{24\mu^{(2)}}\left(\frac{y^5}{5}-yh^4\right)+\frac{B^{(2)}\left(yh^2-\frac{y^3}{3}\right)}{2\mu^{(2)}}-\frac{A^{(2)}\left(\frac{y^4}{4}-yh^3\right)}{6\mu^{(2)}}\\ -\frac{h_1}{\mu^{(2)}}\left(B^{(1)}-B^{(2)}\right)\left(\frac{y^2}{2}-yh\right)+\frac{h_1^2}{2\mu^{(2)}}A^{(2)}\left(\frac{y^2}{2}-hy\right)\end{array}\right).\end{aligned} \tag{2.86}$$

Total volumetric flow in dimensionless form is given by

$$Q = Q^{(1)} + Q^{(2)}, \tag{2.87}$$

$$\begin{aligned}Q &= hu(h)+\frac{1}{3}\frac{dp}{dx}\left(h_1^3\left(\frac{1}{\mu^{(2)}}-\frac{1}{\mu^{(1)}}\right)-\frac{h^3}{\mu^{(2)}}\right)\\ &+Gr_t\left(\begin{array}{c}\frac{\Pr b}{120}\left(4h_1^5\left(\frac{1}{\mu^{(2)}}-\frac{1}{\mu^{(1)}}\right)-\frac{4h^5}{\mu^{(2)}}\right)-\\ \frac{B^{(2)}\left(h_1^3-h^3\right)}{3\mu^{(2)}}-\frac{A^{(2)}\left(h_1^4-h^4\right)}{8\mu^{(2)}}+\frac{h_1^3B^{(1)}}{3\mu^{(1)}}-\\ -\frac{h_1}{2\mu^{(2)}}\left(B^{(1)}-B^{(2)}\right)\left(h_1^2-h^2\right)+\frac{h_1^2}{4\mu^{(2)}}A^{(2)}\left(h_1^2-h^2\right)\end{array}\right).\end{aligned} \tag{2.88}$$

Pressure gradient in terms of volumetric flow is given by

$$\frac{dp}{dx} = 3\left(Q - hu(h) - Gr_t\left(\begin{array}{c} \frac{\Pr b}{120}\left(4h_1^5\left(\frac{1}{\mu^{(2)}} - \frac{1}{\mu^{(1)}}\right) - \frac{4h^5}{\mu^{(2)}}\right) - \\ \frac{B^{(2)}\left(h_1^3 - h^3\right)}{3\mu^{(2)}} - \frac{A^{(2)}\left(h_1^4 - h^4\right)}{8\mu^{(2)}} + \frac{h_1^3 B^{(1)}}{3\mu^{(1)}} - \\ -\frac{h_1}{2\mu^{(2)}}\left(B^{(1)} - B^{(2)}\right)\left(h_1^2 - h^2\right) + \frac{h_1^2}{4\mu^{(2)}}A^{(2)}(h_1^2 - h^2) \end{array}\right)\right) \div \left(h_1^3\left(\frac{1}{\mu^{(2)}} - \frac{1}{\mu^{(1)}}\right) - \frac{h^3}{\mu^{(2)}}\right). \tag{2.89}$$

2.3 Graphical Results

This section provides the effect of flow parameters such as viscosities $\mu^{(1)}$ and $\mu^{(2)}$, thermal buoyancy parameter Gr_t, constant heat radiation factor b and Prandtl number Pr on pressure, streamlines, velocity and temperature profiles.

2.3.1 Velocity Profile

Fig. 2.2 (a-b) shows the decaying effect of viscosity of Newtonian fluid in layer I and II for the axial velocity. The resistive property of the fluid in layer I causes to decelerate the flow near the center but does not change the flow near the cilia tip. But the viscosity of the fluid in layer II gives the decreasing effect in both layers I and II. Fig. 2.2 (c) displays the growing effect of thermal buoyancy parameter Gr_t, on axial velocity, it indicates that when buoyancy force become double, triple, and four times of the inertial force, viscosity of the viscous fluid in both layers reduces that results to increase the flow in both layers. Fig. 2.2 (d) illustrates the effect of Prandtl number on flow field, it indicates that when kinematic viscosity became double, triple and four times of the thermal conductivity of the fluid; the flow rises in both layers I and II. Fig. 2.2 (e) shows the effect of heat radiation parameter on axial flow, it is observed that intensity of radiation factor help to flow fastly in layer I and II, but the flow in layer I has high rate as compared with layer II.

2.3.2 Temperature Profile

Fig. 2.3(a-b) shows the impact of Prandtl number Pr and heat radiation factor b, this figure shows that when kinematic viscosity is dominant over thermal conductivity, then temperature in fluid rises, also the radiation factor causes to increase the temperature in fluid.

2.3.3 Pressure distribution

Fig. 2.4(a-b) displays the variation in favorable pressure for the varying values of volume flow rate and thermal buoyancy parameter Gr_t. It is noted that pressure change during the flow and rises when volume flow increases, similarly when buoyancy force became double, triple and four times of the inertial force then pressure change in fluid flow rises significantly near entry and exit point.

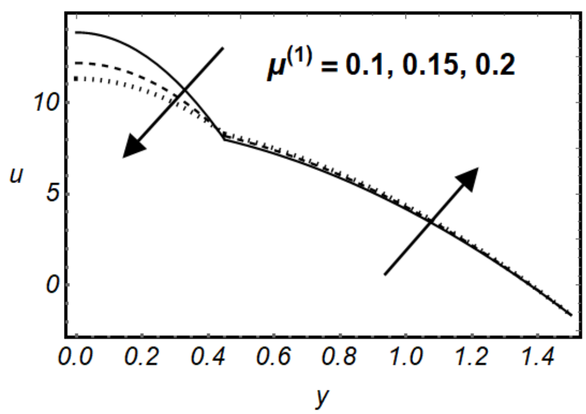

(a)

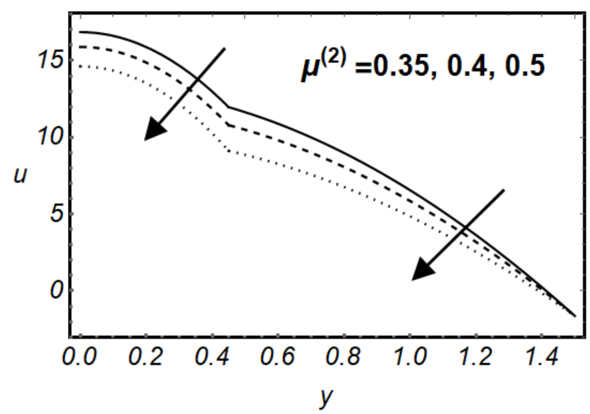

(b)

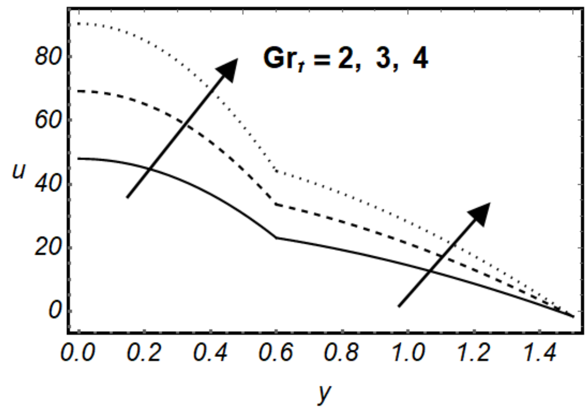

(c)

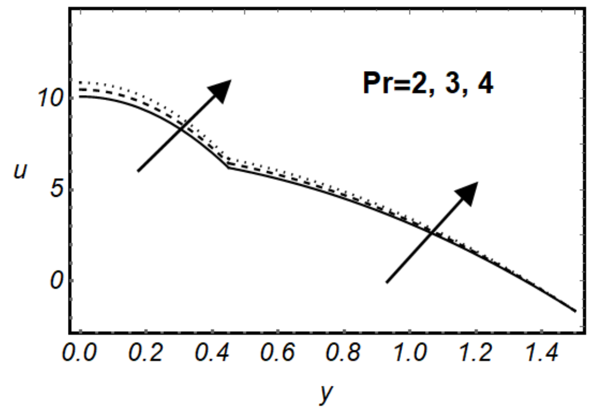

(d)

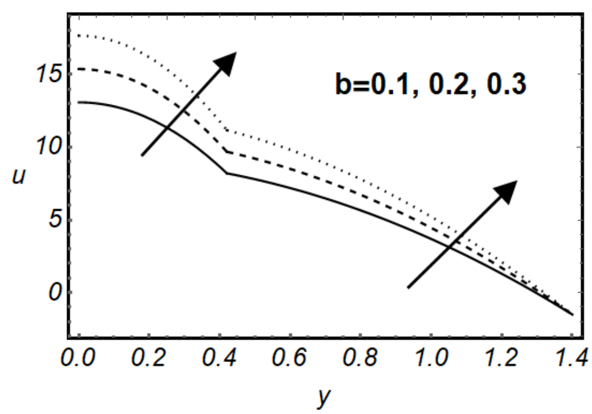

(e)

Fig. 2.2 (a-e): Influence of $\mu^{(1)}$, $\mu^{(2)}$, thermal buoyancy parameter Gr_t, Prandtl number Pr and heat radiation factor b on velocity profile.

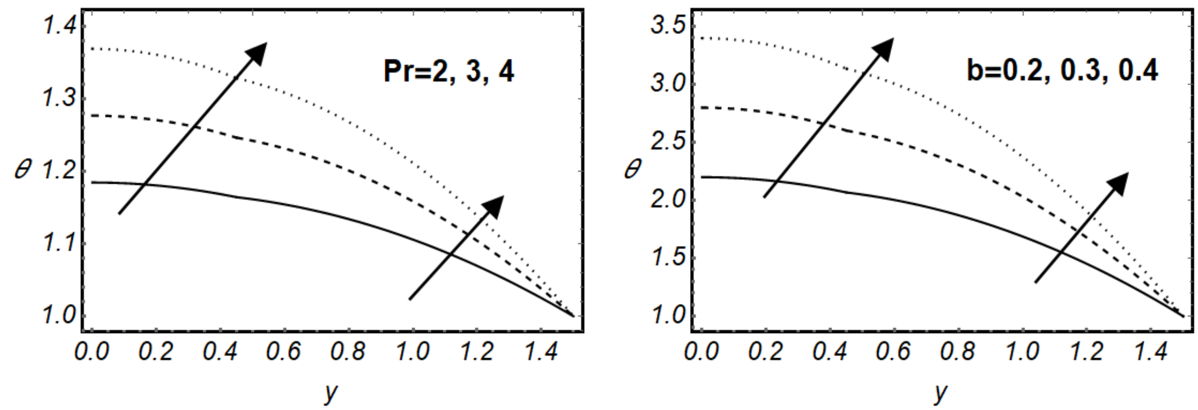

(a) (b)

Fig. 2.3(a-b): Influence of Prandtl number Pr and heat radiation factor b on temperature profile.

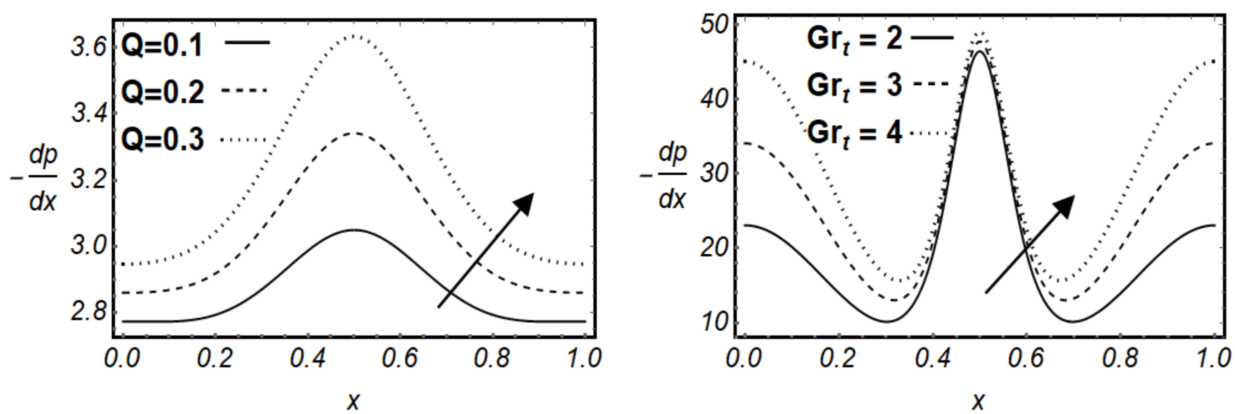

(a) (b)

Fig. 2.4(a-b): Impact of volume flow rate Q and thermal buoyancy parameter Gr_t on pressure gradient.

Chapter 3

Heat Transfer Analysis of Ellis Fluid Flow in a Peripheral Layer

This chapter examines the heat transfer analysis of Ellis fluid flow through a channel that is anchored by cilia. It is assumed that the convective flow is incompressible and immiscible within a conduite and movement in the flow is due to the cilia tip. Mathematical model of the problem provides a complex system of partial differential equations which are simplified by the lubrication approach and solved under the no-slip and fluid interface condition. Mathematical results for velocity, pressure, stream function and temperature are found in an explicit form and displayed the impact of emerging parameters by graphs.

3.1 Formulation of the Problem

For the locomotion of Ellis fluid it is assumed that the flow is generated by the cilia tips that forms back and fro motion causing the metachronal wave. The Cartesian coordinate system is chosen and the parametric equations for the path followed by the cilia tip are given as follows:

$$X^* = f(X^*, X_0^*, t^*) = X_0^* + a\epsilon\alpha \sin\left(2\pi\left(\frac{X^* - ct^*}{\lambda}\right)\right), \tag{3.1}$$

$$Y^* = f^{''}(X^*, t^*) = a + a\epsilon \cos\left(2\pi\left(\frac{X^* - ct^*}{\lambda}\right)\right) \tag{3.2}$$

where ϵ is a non dimensional cilia length parameter, $X_0^*$is the reference position of cilia, α is the eccentricity of elliptical path, λ and c are the wavelength and wave speed of metachronal wave respectively.

The two-layer flow through a ciliated channel suggests the following velocity profile:

$$V^{*(k)} = \left[U^{*(k)}(X^*, Y^*, t^*), V^{*(k)}(X^*, Y^*, t^*), 0\right], \tag{3.3}$$

where $U^{*(k)}$ and $V^{*(k)}$ are the axial and transverse velocity respectively. Superscripts $k = 1, 2$ correspond to layer I ($k = 1$) and layer II ($k = 2$) of the Ellis fluid.

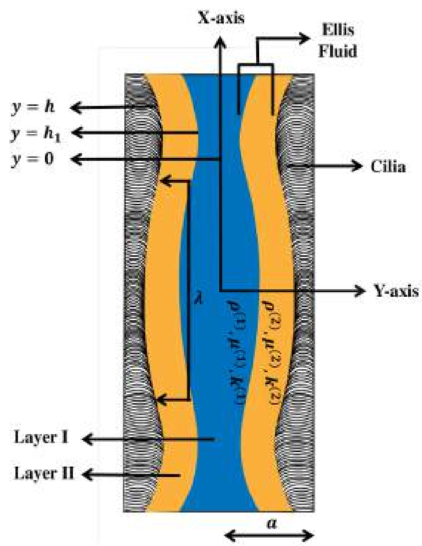

Fig. 3.1: Geometry of the flow problem

The two layer convective flow of viscous fluid through a ciliated channel is governed by the following equations.

$$\boldsymbol{\nabla}.\mathbf{V}^{*(k)} = 0, \tag{3.4}$$

$$\rho^{*(k)} \frac{d\mathbf{V}^{*(k)}}{dt^*} = \text{div}\,\boldsymbol{\tau}^{(k)} + \rho^{*(k)}\mathbf{b}, \tag{3.5}$$

$$\rho^{*(k)} c_p^{(k)} \frac{dT^{*(k)}}{dt^*} = K^{(k)} \boldsymbol{\nabla}^2 T^{(k)} + Q_0, \tag{3.6}$$

where $\rho^{*(k)}$ denotes density, $\boldsymbol{\tau}^{(k)}$ is stress tensor for Ellis fluid in both layers and are given as follows:

$$\boldsymbol{\tau}^{(k)} = -P^{*}I + S, \tag{3.7}$$

$$S = \left(\frac{\mu^{(k)}}{1 + \left(\frac{L_s^{(k)}}{S_0^{(k)}} \right)^{\alpha - 1}} \right) A_1^{(k)}, \tag{3.8}$$

$$A_1 = \boldsymbol{\nabla} \mathbf{V}^{*(k)} + \left(\boldsymbol{\nabla} \mathbf{V}^{*(k)} \right)^{t}, \tag{3.9}$$

$$S_0^{(k)} = \frac{\mu^{(k)}}{2}, \tag{3.10}$$

$$L_s^{(k)} = \sqrt{\frac{1}{2} t_r \left(A_1^{(k)} \right)^2}, \tag{3.11}$$

$P^{*}$is the pressure, I represents identity matrix, S is the extra stress tensor for an Ellis Fluid, $\mu^{(k)}$ is the dynamic viscosity, $S_0^{(k)}$and α are material constants, $L_s^{(k)}$ is second order invariant of stress tensor and $A_1^{(k)}$is the first Rivilian Erickson tensor, $c_p^{(k)}$ gives specific heat at constant pressure, $K^{(1)}$ and $K^{(2)}$ is thermal conductivity and Q_0 reflects heat source term.

In layer I and II, no slip conditions suggest that the fluid particles lying adjacent to cilia tips moves with speed of cilia tips. Therefore, the velocity at the boundary is given as follows:

$$U^{*(k)} = \frac{\partial f}{\partial t^{*}} + \frac{\partial f}{\partial X^{*}} \frac{\partial X^{*}}{\partial t^{*}} = \frac{\partial f}{\partial t^{*}} + \frac{\partial f}{\partial X^{*}} U^{*}, \tag{3.12}$$

$$V^{*(k)} = \frac{\partial f''}{\partial t^{*}} + \frac{\partial f''}{\partial X^{*}} \frac{\partial X^{*}}{\partial t^{*}} = \frac{\partial f''}{\partial t^{*}} + \frac{\partial f''}{\partial X^{*}} U^{*}. \tag{3.13}$$

Using Eqs.(3.1)-(3.2) in Eqs.(3.12)-(3.13) one can get following form of velocity at the boundary:

$$U^{*} = \frac{-\frac{2\pi}{\lambda} \epsilon \alpha a c \cos\left(2\pi \left(\frac{X^{*} - ct^{*}}{\lambda}\right)\right)}{1 - \frac{2\pi}{\lambda} \epsilon \alpha c a \cos\left(2\pi \left(\frac{X^{*} - ct^{*}}{\lambda}\right)\right)}, \tag{3.14}$$

$$V^{*} = \frac{\frac{2\pi}{\lambda} \epsilon a c \sin\left(2\pi \left(\frac{X^{*} - ct^{*}}{\lambda}\right)\right)}{1 - \frac{2\pi}{\lambda} \epsilon \alpha a \cos\left(2\pi \left(\frac{X^{*} - ct^{*}}{\lambda}\right)\right)}, \tag{3.15}$$

where U^{*} and V^{*} are the velocity components at the following wavy boundary:

$$Y^{*} = \pm a \left(1 + \epsilon \cos\left(2\pi \left(\frac{X^{*} - ct^{*}}{\lambda} \right) \right) \right). \tag{3.16}$$

To transform the fixed frame (X^*, Y^*, t^*) into wave frame (x^*, y^*), following relations are used:

$$p^*(x^*, y^*) = P^*(X^*, Y^*, t^*), y^* = Y^*, x^* = X^* - ct^*, v^* = V^*, u^* = U^* - c \tag{3.17}$$

To describe the convective flow of Ellis fluid between the two layers following laws are used:

$$\frac{\partial u^{*(k)}}{\partial x^*} + \frac{\partial v^{*(k)}}{\partial y^*} = 0, \tag{3.18}$$

$$\rho^{*(k)} \left(\left(u^{*(k)} + c \right) \frac{\partial u^{*(k)}}{\partial x^*} + v^{*(k)} \frac{\partial u^{*(k)}}{\partial y^*} \right) = -\frac{\partial p^*}{\partial x^*} + \frac{\partial \tau_{xx}^{*(k)}}{\partial x^*} + \frac{\partial \tau_{xy}^{*(k)}}{\partial y^*} + \rho^{(k)} g\beta(T^* - T_0^*), \tag{3.19}$$

$$\rho^{*(k)} \left(\left(u^{*(k)} + c \right) \frac{\partial v^{*(k)}}{\partial x^*} + v^{*(k)} \frac{\partial v^{*(k)}}{\partial y^*} \right) = -\frac{\partial p^*}{\partial y^*} + \frac{\partial \tau_{yx}^{*(k)}}{\partial x^*} + \frac{\partial \tau_{yy}^{*(k)}}{\partial y^*}, \tag{3.20}$$

$$\rho^{*(k)} c_p^{(k)} \left(\left(u^{*(k)} + c \right) \frac{\partial T^{*(k)}}{\partial x^*} + v^{*(k)} \frac{\partial T^{*(k)}}{\partial y^*} \right) = K^{(k)} \left(\frac{\partial^2 T^{*(k)}}{\partial x^{*2}} + \frac{\partial^2 T^{*(k)}}{\partial y^{*2}} \right) + Q_0, \tag{3.21}$$

$$\tau_{xy}^{*(k)} = \frac{\mu^{*(k)}}{R^{*(k)}} \left(\frac{\partial v^{*(k)}}{\partial x^*} + \frac{\partial u^{*(k)}}{\partial y^*} \right), \tag{3.22}$$

$$\tau_{xx}^{*(k)} = \frac{2\mu^{*(k)}}{R^{*(k)}} \frac{\partial u^{*(k)}}{\partial x^*}, \tag{3.23}$$

$$\tau_{yy}^{*(k)} = \frac{2\mu^{*(k)}}{R^{*(k)}} \frac{\partial v^{*(k)}}{\partial y^*}, \tag{3.24}$$

where,

$$R^{*(k)} = 1 + \left(\frac{\sqrt{2\left(\left(\frac{\partial u^{*(k)}}{\partial x^*} \right)^2 + \left(\frac{\partial v^{*(k)}}{\partial y^{*(k)}} \right)^2 \right) + \left(\frac{\partial u^{*(k)}}{\partial y^*} + \frac{\partial v^{*(k)}}{\partial x^{*(k)}} \right)^2}}{\frac{\mu^{*(k)}}{2}} \right)^{\alpha - 1}. \tag{3.25}$$

Since the biological flows are Poiseuille type, therefore flow and temperature are assumed to be maximum at center line $y = 0$ and fluid interface implies the following conditions:

$$\tau_{xy}^{*(1)} = 0, \text{ at } y^* = 0, \tag{3.26}$$

$$\tau_{xy}^{*(1)} = \tau_{xy}^{*(2)}, \text{ at } y^* = h_1^*, \tag{3.27}$$

$$u^{*(1)} = u^{*(2)}, \text{ at } y^* = h_1^*, \tag{3.28}$$

$$u^{*(2)} + c = \frac{-\frac{2\pi}{\lambda}\epsilon\alpha ac\cos\left(\frac{2\pi x^*}{\lambda}\right)}{1 - \frac{2\pi}{\lambda}\epsilon\alpha ac\cos\left(\frac{2\pi x^*}{\lambda}\right)}, \text{ at } y^* = h^*, \tag{3.29}$$

$$v^{*(2)} = \frac{\frac{2\pi}{\lambda}\epsilon ac\sin\left(\frac{2\pi x^*}{\lambda}\right)}{1 - \frac{2\pi}{\lambda}\epsilon\alpha a\cos\left(\frac{2\pi x^*}{\lambda}\right)}, \text{ at } y^* = h^*. \tag{3.30}$$

Temperature at the fluid interface implies the following conditions

$$\frac{\partial T^{*(k)}}{\partial y^*} = 0, \text{ at } y^* = 0, \tag{3.31}$$

$$K^{(1)}\frac{\partial T^{*(1)}}{\partial y^*} = K^{(2)}\frac{\partial T^{*(2)}}{\partial y^*}, at\ y^* = h_1^*, \tag{3.32}$$

$$T^{*(1)} = T^{*(2)}, \ at\ y^* = h_1^*, \tag{3.33}$$

$$T^{*(2)} = T_1, \text{ at } y^* = h^*, \tag{3.34}$$

where,

$$h^* = \pm\left(a + a\epsilon\cos\left(\frac{2\pi x^*}{\lambda}\right)\right), \tag{3.35}$$

$$h_1^* = \pm\left(a + a\epsilon\cos\left(\frac{2\pi x^*}{\lambda}\right)\right). \tag{3.36}$$

Non dimensional parameters are introduced as follows:

$$\begin{aligned}
x &= \frac{x^*}{\lambda},\ y = \frac{y^*}{a},\ u^{(k)} = \frac{u^{*(k)}}{c},\ v^{(k)} = \frac{v^{*(k)}}{\gamma c},\ h = \frac{h^*}{a},\ h_1 = \frac{h_1^*}{a},\ p = \frac{a\gamma}{c\mu^{(1)}}p^*,\ \gamma = \frac{a}{\lambda}, \\
\text{Re} &= \frac{\rho ac}{\mu^{(1)}},\ \text{Pr} = \frac{\mu^{(1)}c_p}{k^{(k)}},\ \theta = \frac{T^{*(k)} - T_0^*}{T_1^* - T_0^*},\ \rho^{(k)} = \frac{\rho^{*(k)}}{\rho^{(1)}},\ \mu^{(k)} = \frac{\mu^{*(k)}}{\mu^{(1)}},\ k^{(k)} = \frac{k^{*(k)}}{k^{(1)}}, \\
Gr &= \frac{ga^3\beta(T_1^* - T_0^*)}{\nu^2},\ b = \frac{a^2Q_0}{(T_1^* - T_0^*)\mu^{(1)}c_p},\ \delta = \frac{a_1}{a},\ Gr_t = \frac{Gr}{\text{Re}},\ \tau_{ij}^{(k)} = \frac{a}{c\mu^{(1)}}\tau_{ij}^{*(k)}, \\
\beta &= \left(\frac{c}{a\mu^{(k)}\mu^{(1)}}\right)^{\alpha-1}.
\end{aligned} \tag{3.37}$$

Using above parameters Eqs. (3.19)-(3.36) reduce into the following form.

$$\frac{\partial u^{(k)}}{\partial x} + \frac{\partial v^{(k)}}{\partial y} = 0, \tag{3.38}$$

$$\operatorname{Re}\gamma\left(\left(u^{(k)}+1\right)\frac{\partial u^{(k)}}{\partial x}+v^{(k)}\frac{\partial u^{(k)}}{\partial y}\right)=-\frac{\partial p}{\partial x}+\gamma\frac{\partial\tau_{xx}^{(k)}}{\partial x}+\frac{\partial\tau_{xy}^{(k)}}{\partial y}+Gr_t\theta^{(k)}, \tag{3.39}$$

$$\operatorname{Re}\gamma^3\left(\left(u^{(k)}+1\right)\frac{\partial v^{(k)}}{\partial x}+v^{(k)}\frac{\partial v^{(k)}}{\partial y}\right)=-\frac{\partial p}{\partial y}+\gamma^2\frac{\partial\tau_{yx}^{(k)}}{\partial x}+\gamma\frac{\partial\tau_{yy}^{(k)}}{\partial y}, \tag{3.40}$$

$$\operatorname{Pr}\operatorname{Re}\gamma\left(\left(u^{(k)}+1\right)\frac{\partial\theta^{(k)}}{\partial x}+v^{(k)}\frac{\partial\theta^{(k)}}{\partial y}\right)=\gamma^2\left(\frac{\partial^2\theta^{(k)}}{\partial x^2}+\frac{\partial^2\theta^{(k)}}{\partial y^2}\right)+\operatorname{Pr}b, \tag{3.41}$$

$$\tau_{xy}^{(k)}=\frac{\mu^{(k)}}{R^{(k)}}\left(\gamma^2\frac{\partial v^{(k)}}{\partial x}+\frac{\partial u^{(k)}}{\partial y}\right), \tag{3.42}$$

$$\tau_{xx}^{(k)}=\frac{2\gamma\mu^{(k)}}{R^{(k)}}\frac{\partial u^{(k)}}{\partial x}, \tag{3.43}$$

$$\tau_{yy}^{(k)}=\frac{2\gamma\mu^{(k)}}{R^{(k)}}\frac{\partial v^{(k)}}{\partial y}. \tag{3.44}$$

Non-dimensional boundary conditions at fluid interface are given as:

$$\tau_{xy}^{(1)}=0,\ \text{at}\ y=0, \tag{3.45}$$

$$\tau_{xy}^{(1)}=\tau_{xy}^{(2)},\ \text{at}\ y=h_1, \tag{3.46}$$

$$u^{(1)}=u^{(2)},\ \text{at}\ y=h_1, \tag{3.47}$$

$$u^{(2)}=\frac{-2\pi\epsilon\alpha\gamma\cos(2\pi x)}{1-2\pi\epsilon\alpha\gamma\cos(2\pi x)}-1,\ \text{at}\ y=h, \tag{3.48}$$

$$v^{(2)}=\frac{2\pi\epsilon\gamma c\sin(2\pi x)}{1-2\pi\epsilon\alpha\gamma\cos(2\pi x)},\ \text{at}\ y=h. \tag{3.49}$$

Non-dimensional form of temperature distribution at fluid interface is as follows:

$$\frac{\partial\theta^{(1)}}{\partial y}=0,\ \text{at}\ y=0, \tag{3.50}$$

$$K^{(1)}\frac{\partial\theta^{(1)}}{\partial y}=K^{(2)}\frac{\partial\theta^{(2)}}{\partial y},\ \text{at}\ y=h_1, \tag{3.51}$$

$$\theta^{(1)}=\theta^{(2)},\ \text{at}\ y=h_1, \tag{3.52}$$

$$\theta^{(2)}=1,\ \text{at}\ y=h, \tag{3.53}$$

where

$$h = \pm \left(1 + \epsilon \cos\left(2\pi x\right)\right), \tag{3.54}$$

$$h_1 = \pm \delta \left(1 + \epsilon \cos\left(2\pi x\right)\right). \tag{3.55}$$

The lubrication approach reduces the Eqs.(3.39-3.49), into following form

$$-\frac{\partial p}{\partial x} + \frac{\partial \tau_{xy}^{(k)}}{\partial y} + Gr_t \theta^{(k)} = 0, \tag{3.56}$$

$$-\frac{\partial p}{\partial y} = 0, \;\; \left(p \neq p(x)\right), \tag{3.57}$$

$$\frac{\partial^2 \theta^{(k)}}{\partial y^2} + \Pr b = 0, \tag{3.58}$$

$$\tau_{xy}^{(k)} = \frac{\mu^{(k)}}{R^{(k)}} \frac{\partial u^{(k)}}{\partial y}, \tag{3.59}$$

$$\tau_{xx}^{(k)} = 0, \tag{3.60}$$

$$\tau_{yy}^{(k)} = 0, \tag{3.61}$$

with boundary conditions

$$\tau_{xy}^{(1)} = 0, \text{ at } y = 0, \tag{3.62}$$

$$\tau_{xy}^{(1)} = \tau_{xy}^{(2)}, \text{ at } y = h_1, \tag{3.63}$$

$$u^{(1)} = u^{(2)}, \text{ at } y = h_1, \tag{3.64}$$

$$u^{(2)} = -2\pi\epsilon\alpha\gamma \cos\left(2\pi x\right) - 1, \text{ at } y = h, \tag{3.65}$$

$$v^{(2)} = 2\pi\epsilon\gamma \sin\left(2\pi x\right) + \left(2\pi\epsilon\gamma\right)^2 \alpha \sin\left(2\pi x\right) \cos\left(2\pi x\right), \text{ at } y = h. \tag{3.66}$$

where

$$R^{(k)} = 1 + \beta \left(\frac{\partial u^{(k)}}{\partial y}\right)^{\alpha - 1} \tag{3.67}$$

$$\beta = \left(\frac{c}{a\mu^{(k)}\mu^{(1)}}\right)^{\alpha - 1}, \tag{3.68}$$

where, β is Ellis fluid parameter.

Temperature profile at boundary is given by

$$\frac{\partial \theta^{(1)}}{\partial y} = 0, \text{ at } y = 0, \tag{3.69}$$

$$K^{(1)} \frac{\partial \theta^{(1)}}{\partial y} = K^{(2)} \frac{\partial \theta^{(2)}}{\partial y}, \text{ at } y = h_1, \tag{3.70}$$

$$\theta^{(1)} = \theta^{(2)}, \text{ at } y = h_1, \tag{3.71}$$

$$\theta^{(2)} = 1, \text{ at } y = h. \tag{3.72}$$

3.2 Solution of the Problem

Integrating Eq. (3.58) one can get the temperature profile as follows

$$\theta^{(k)} = -\frac{\Pr b y^2}{2} + A^{(k)} y + B^{(k)}, \tag{3.73}$$

where $A^{(k)}$ and $B^{(k)}$ are constants of integration, that can be found by the boundary conditions given in Eqs. (3.69)-(3.72)

$$A^{(1)} = 0, \ 0 \leq y \leq h_1, \tag{3.74}$$

$$B^{(1)} = 1 + \Pr b \left(\left(1 - \frac{k^{(1)}}{k^{(2)}} \right) h_1 \left(h_1 - h \right) + \frac{h^2}{2} \right), \ 0 \leq y \leq h_1, \tag{3.75}$$

$$A^{(2)} = \left(1 - \frac{k^{(1)}}{k^{(2)}} \right) \Pr b h_1, \ h_1 \leq y \leq h, \tag{3.76}$$

$$B^{(2)} = 1 + \Pr b h \left(\frac{h}{2} - h_1 \left(1 - \frac{k^{(1)}}{k^{(2)}} \right) \right) \ h_1 \leq y \leq h. \tag{3.77}$$

Using Eqs. (3.74-3.77) in Eq. (3.73) one can get the temperature profiles for two regions which can be written as follows

$$\theta^{(1)} = 1 - \Pr b \left(\frac{\left(y^2 - h^2 \right)}{2} - \left(1 - \frac{k^{(1)}}{k^{(2)}} \right) h_1 \left(h_1 - h \right) \right), \tag{3.78}$$

$$\theta^{(2)} = 1 - \Pr b \left(\frac{\left(y^2 - h^2 \right)}{2} - \left(1 - \frac{k^{(1)}}{k^{(2)}} \right) h_1 \left(y - h \right) \right). \tag{3.79}$$

Rewrite Eq.(3.56) in the presence of body force

$$\frac{\partial \tau_{xy}^{(1)}}{\partial y} = \frac{dp}{dx} - Gr_t \theta^{(1)} \tag{3.80}$$

$$\frac{\partial \tau_{xy}^{(2)}}{\partial y} = \frac{dp}{dx} - Gr_t \theta^{(2)}. \tag{3.81}$$

Upon integrating Eqs. (3.81) w.r.t y and using boundary conditions (3.62-3.63), one can get following expressions for shear stress:

$$\tau_{xy}^{(1)} = \frac{dp}{dx} y - Gr_t \left(-\frac{\Pr b}{6} y^3 + B^{(1)} y \right), \ 0 \leq y \leq h_1 \tag{3.82}$$

$$\tau_{xy}^{(2)} = \frac{dp}{dx} y - Gr_t \left(-\frac{\Pr b}{6} y^3 + \frac{y^2}{2} A^{(2)} + B^{(2)} y \right) + c^{(2)}, \ h_1 \leq y \leq h, \tag{3.83}$$

where

$$c^{(2)} = Gr_t h_1 \left(B^{(2)} - B^{(1)} + \frac{h_1}{2} A^{(2)} \right). \tag{3.84}$$

After simplifying and integrating Eqs. (3.82-3.83) w.r.t y, and using Eq. (3.59), one can get the following expressions:

$$u^{(k)} = \mu^{(k)} \int_0^h \tau_{xy}^{(k)} R^{(k)} dy, \tag{3.85}$$

or

$$u^{(k)} = \mu^{(1)} \int_0^{h_1} \tau_{xy}^{(1)} R^{(1)} dy + \mu^{(2)} \int_{h_1}^{h} \tau_{xy}^{(2)} R^{(2)} dy. \tag{3.86}$$

Applying boundary conditions given in Eqs.(3.64-3.65), one can get following axial velocity for both regions,

$$u^{(1)} = u(h) + f_1 + \left(\frac{dp}{dx} \right)^2 f_2 + \left(\frac{dp}{dx} \right) f_3 + Gr_t \left[f_4 + \beta(f_5) \right], \tag{3.87}$$

$$u^{(2)} = u(h) + g_1 + \left(\frac{dp}{dx} \right)^2 g_2 + \left(\frac{dp}{dx} \right) g_3 + Gr_t \left[g_4 - \frac{\beta}{\mu^{(2)}} (g_5) \right]. \tag{3.88}$$

To find the transverse component of velocity, following form of Eq.(3.38)is used:

$$\frac{\partial v^{(k)}}{\partial y} = -\frac{\partial u^{(k)}}{\partial x}, \tag{3.89}$$

Integrating above equation w.r.t y and solving for $v^{(k)}$ and using no slip boundary condition, one can get following expressions:

$$v^{(1)} = v(h) - f_6 - \left(\frac{d^2p}{dx^2}\right)\left[2\left(\frac{dp}{dx}\right) f_7 + f_8 + \beta Gr_t(f_9)\right], \tag{3.90}$$

$$v^{(2)} = v(h) - f_6 - \left(\frac{d^2p}{dx^2}\right)\left[2\left(\frac{dp}{dx}\right) g_6 + \frac{1}{\mu^{(2)}}\left\{g_7 + \frac{\beta Gr_t}{\mu^{(2)}}(g_8)\right\}\right]. \tag{3.91}$$

Following relation of stream function helps to find the flow patterns of Ellis fluid:

$$\frac{\partial \psi^{(k)}}{\partial y} = u^{(k)}, \tag{3.92}$$

$$\frac{\partial \psi^{(k)}}{\partial x} = -v^{(k)}. \tag{3.93}$$

Using Eqs. (3.92-3.93), for $k = 1$ (layer 1) and $k = 2$ (layer 2), one can get stream functions for layer I and II, which are given as follows:

$$\psi^{(1)} = -\int v(h)dx + f_{10} + f_1 y + \left(\frac{dp}{dx}\right)^2 f_7 + \left(\frac{dp}{dx}\right)\{\, f_8 + \beta Gr_t\,(f_9)\} + Gr_t\ f_{11}, \tag{3.94}$$

$$\psi^{(2)} = -\int v(h)dx + f_{10} + g_9 + \left(\frac{dp}{dx}\right)^2 g_6 + \frac{1}{\mu^{(2)}}\left(\frac{dp}{dx}\right)\left(g_7 + \frac{\beta Gr_t}{\mu^{(2)}} g_8\right) + \frac{Gr_t}{\mu^{(2)}}\left[g_{10} - \frac{\beta}{\mu^{(2)}} g_{11}\right]. \tag{3.95}$$

Total volumetric flow in dimensionless form is given by

$$Q = Q^{(1)} + Q^{(2)}, \tag{3.96}$$

$$Q = u(h)h + \left(\frac{dp}{dx}\right)^2 g_{12} + \left(\frac{dp}{dx}\right) g_{13} + f_{12} + Gr_t\ f_{13}. \tag{3.97}$$

Since the volumetric flow Q is in the form of quadratic equation in $\frac{dp}{dx}$, so we use quadratic formula to find the roots of pressure gradient. Following are the roots of $\frac{dp}{dx}$.

$$\frac{dp}{dx} = h_1, h_2, \tag{3.98}$$

where,

$$h_1 = -\left[u(h)h - Q + f_{12} + Gr_t\ f_{13}\right], \tag{3.99}$$

$$h_2 = \frac{-g_{13}}{g_{12}} + u(h)h - Q + f_{12} + Gr_t\ f_{13}. \tag{3.100}$$

where f_{12}, f_{13}, g_{12} and g_{13} are defined in appendix.

3.3 Graphical Results

This section provides the impact of flow parameters, including viscosities $\mu^{(1)}$ and $\mu^{(2)}$, thermal buoyancy parameter Gr_t, constant heat radiation factor b, and Prandtl number Pr, on pressure gradient, stream lines temperature and velocity profiles, with $\delta = 0.5$, $\epsilon = 0.5$, $\alpha = 0.4$, $x = 1$, $\gamma = 0.5$, $b = 0.2$, $k^{(1)} = 0.5$, and $k^{(2)} = 0.6$.

3.3.1 Velocity Profile

Fig. 3.2 (a-b) displays the decaying effect of viscosity on axial velocity in both layers I and II. The viscosity of the fluid in layer I and II reduces the flow in axial direction due to the thickening of the fluid but the magnitude of the velocity is high when viscosity of the fluid in layer I is fixed but viscosity of the fluid in layer II is varying. Fig. 3.2 (c-e) display the growing effect of thermal buoyancy parameter Gr_t, Prandtl number and heat radiation factor on axial velocity of Ellis fluid. It is observed, when kinematic viscosity is seven, eight and nine times of the thermal conductivity of the fluid, then flow rises in the direction of metachronal wave in both layers. The radiation factor also causes to rise the flow in both layers along the length of the channel.

3.3.2 Temperature Profile

Fig. 3.3(a-b) predict the behavior of temperature in the Ellis fluid for the rising values of Prandtl number and heat radiation factor. The temperature of the fluid became high when kinematic viscosity is dominant over thermal conductivity. It is also noticed that intensity of heat radiation factor causes to accelerate the flow in both layers.

3.3.3 Pressure Gradient

Fig. 3.4 (a-b) displays the variation in adverse pressure gradient for varying values of volume flow rate and thermal buoyancy parameter Gr_t. It can be seen that pressure change during the flow increases due to ascending values of volumetric flow rate and it descends by the rising values of thermal buoyancy parameter Gr_t.

3.3.4 Stream lines

Fig. 3.5 (a-f) displays the effect of viscosity of fluid present in layer II in both regions $0 \leq y \leq 0.4$ and $0.4 \leq y \leq 1.4$. In region $0 \leq y \leq 0.4$, the bolus size near the fluid interface $y = 0.4$ rises and number of boluses decreases due to no slip, also near the ciliary tip, the number of boluses and bolus size grow due to no slip between the fluid and wave speed of ciliary tip. Fig. 3.6 (a-f) displays the effect of thermal buoyancy parameter Gr_t, on fluid pattern in both layer I and II. The number of boluses and size of boluses rise near the center line ($y = 0$) of the channel in region $0 \leq y \leq 0.4$, but number of boluses increases near the ciliary tip in region $0.4 \leq y \leq 1.4$. Fig. 3.7 (a-f) shows that Ellis fluid parameter β causes to increase the bolus size near the interface $y = 0.4$ in the region $0 \leq y \leq 0.4$, but decays the bolus size near the ciliary tip in the region $0.4 \leq y \leq 1.4$.

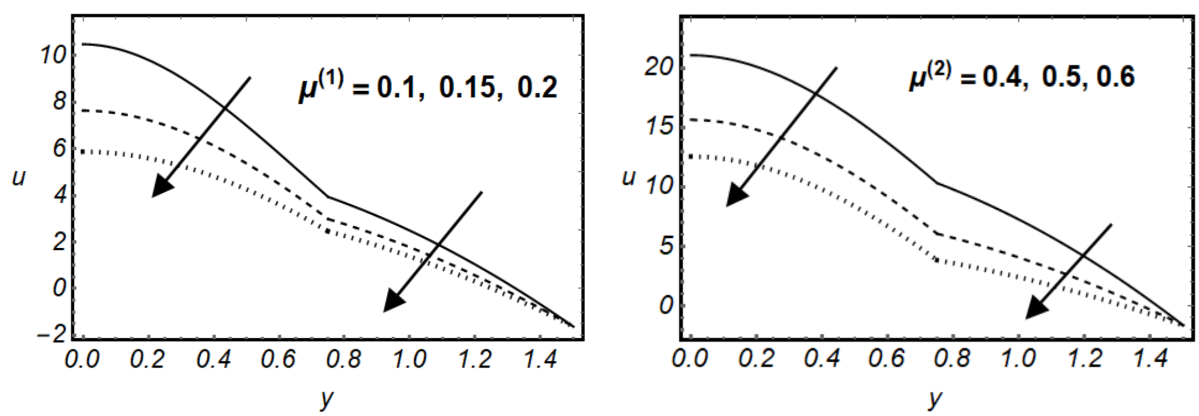

(a) (b)

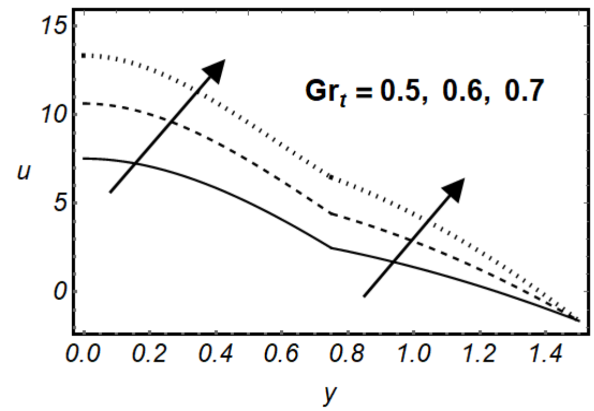

(c)

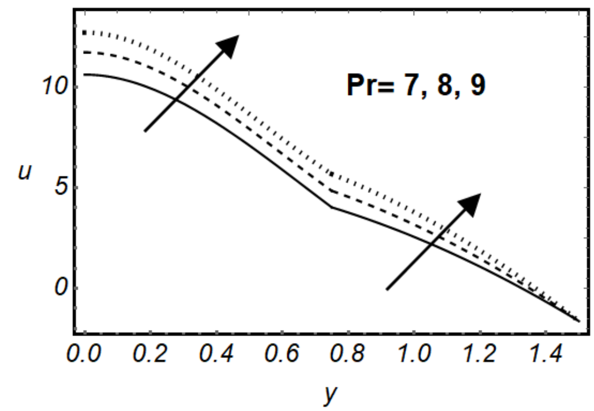

(d)

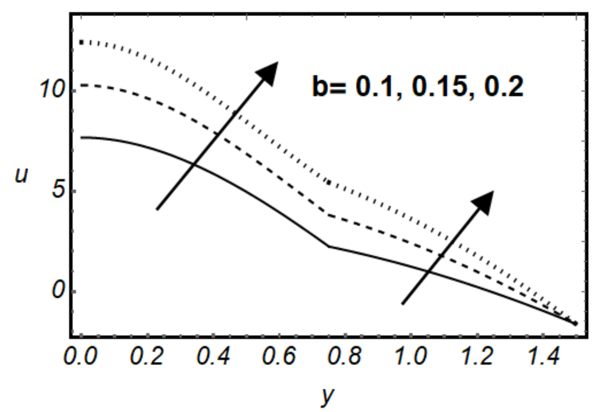

(e)

Fig. 3.2(a-e): Influence of $\mu^{(1)}$, $\mu^{(2)}$, thermal buoyancy parameter Gr_t,Prandtl number Pr and heat radiation factor b on horizontal velocity component.

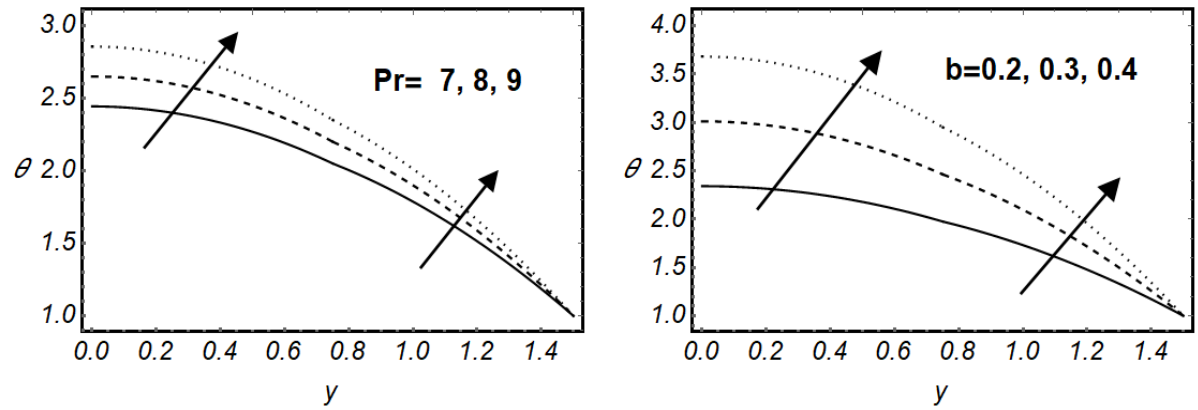

(a) (b)

Fig. 3.3(a-b): Influence of Prandtl number Pr and heat radiation factor b on Temperature profile.

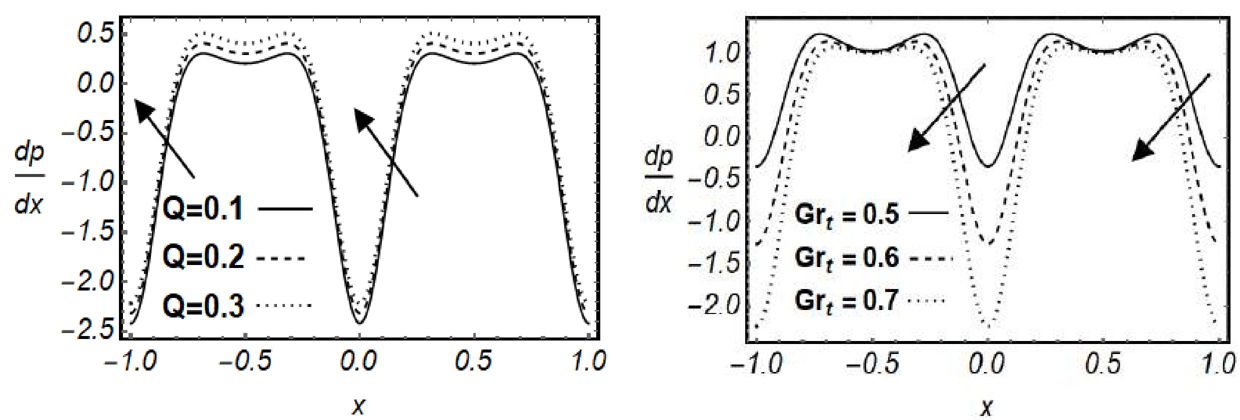

(a) (b)

Fig. 3.4(a-b): Impact of volume flow rate Q and thermal buoyancy parameter Gr_t on pressure gradient.

For stream lines we have considered Ellis fluid parameter ($\beta = 0.2$) in both layers and drawn graphs for layer 1 and layer 2 separately.

Layer 1

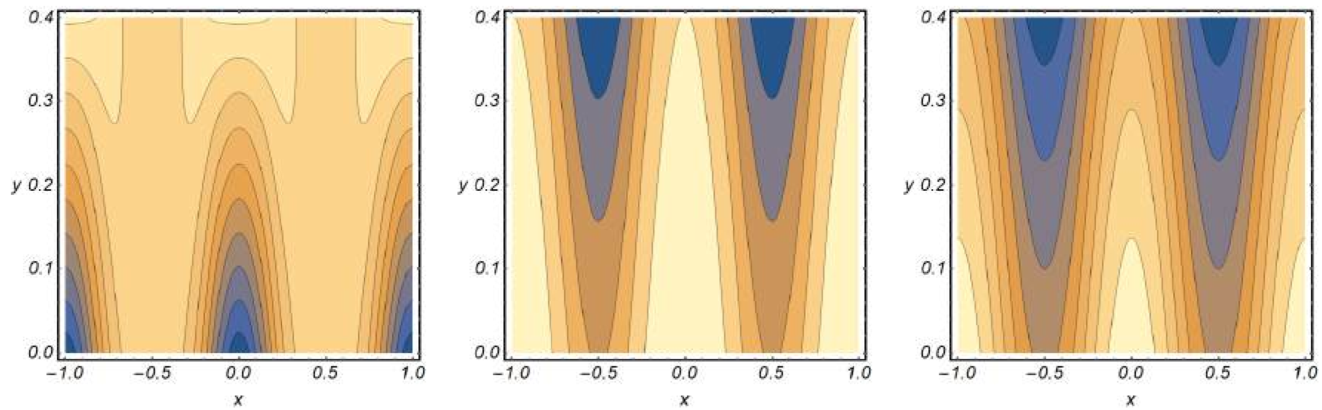

(a) (b) (c)

Layer 2

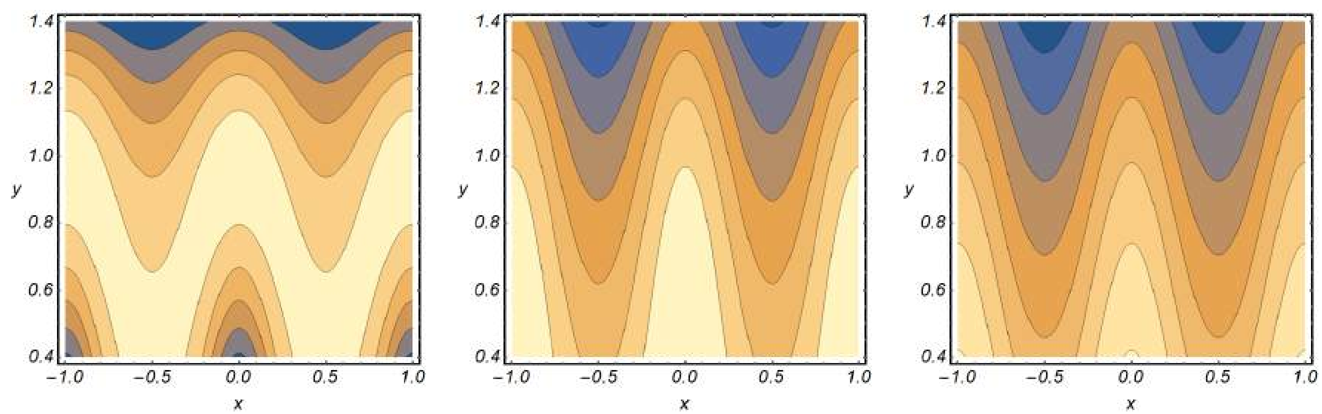

(d) (e) (f)

Fig. 3.5: Variation in $\psi^{(1)}$ for (a) $\mu^{(2)} = 0.4$, (b) $\mu^{(2)} = 0.6$, (c) $\mu^{(2)} = 0.8$ and in $\psi^{(2)}$ for (d) $\mu^{(2)} = 0.4$, $(e)\mu^{(2)} = 0.6$, (f) $\mu^{(2)} = 0.8$.

Layer 1

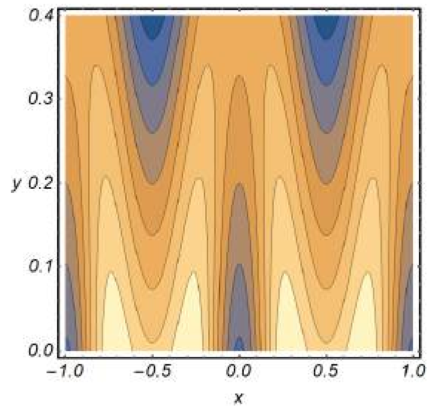

(a)

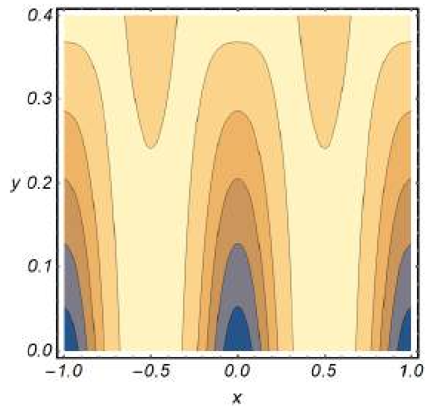

(b)

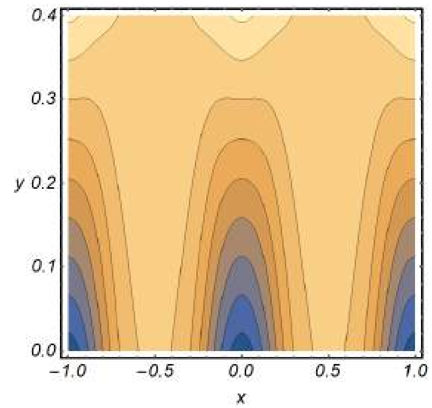

(c)

Layer 2

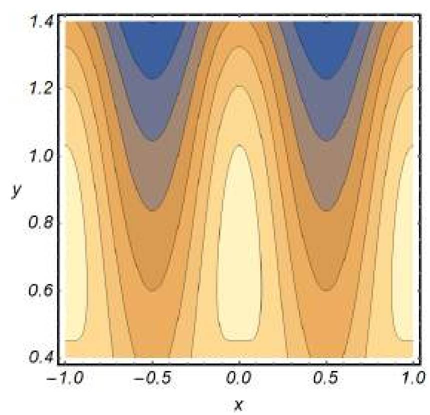

(d)

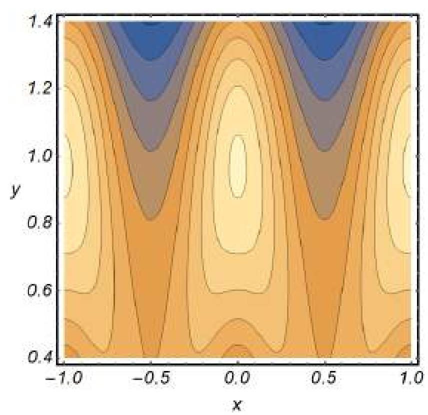

(e)

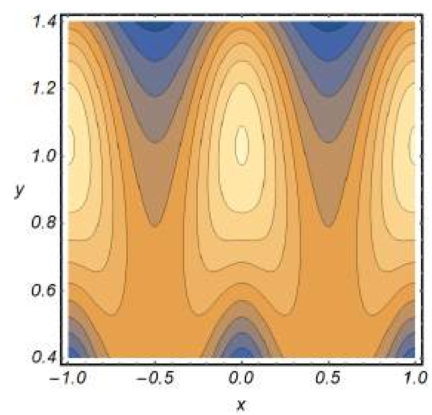

(f)

Fig. 3.6: Variation in $\psi^{(1)}$ for (a) $Gr_t = 0.4$, (b) $Gr_t = 0.5$, $(c) Gr_t = 0.6$ and in $\psi^{(2)}$ for (d) $Gr_t = 0.4$, $(e) Gr_t = 0.5$, (f) $Gr_t = 0.6$.

Layer 1

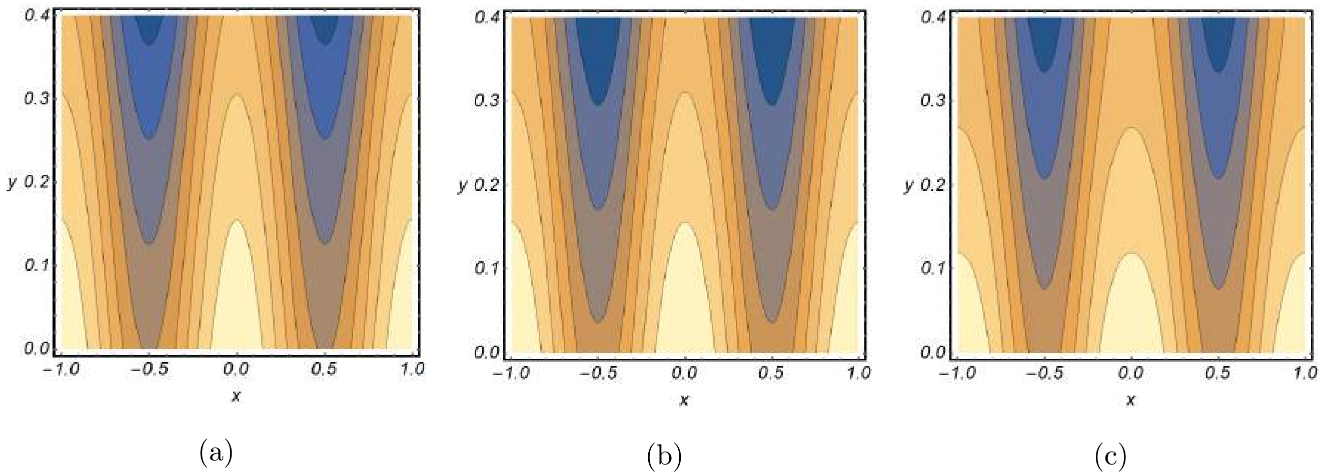

Layer 2

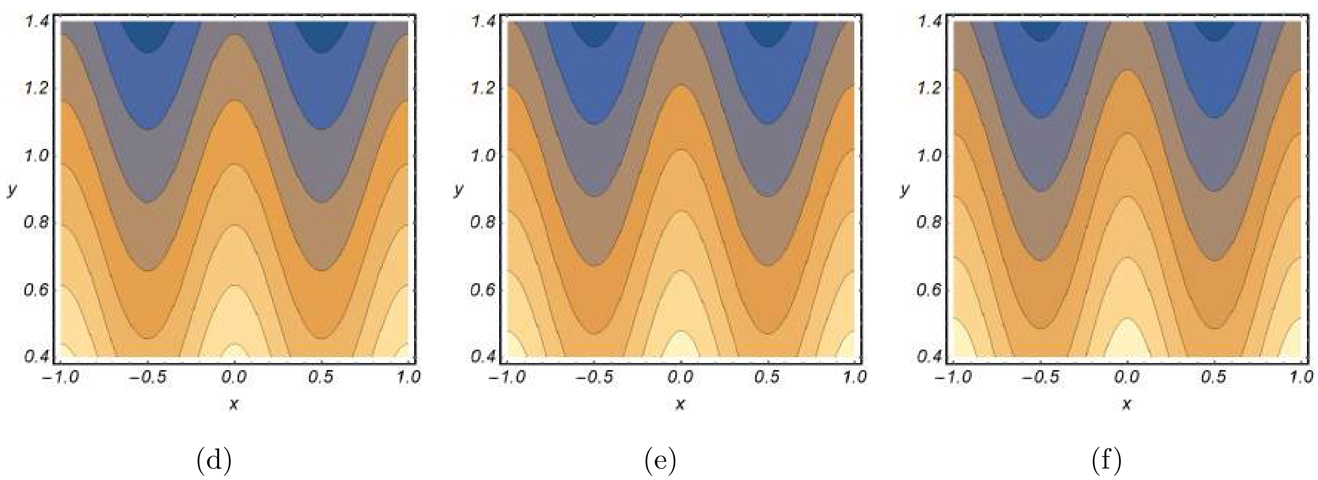

Fig. 3.7: Variation in $\psi^{(1)}$ for (a) $\beta = 0.3$, (b) $\beta = 0.5$, $(c)\beta = 0.7$ and in $\psi^{(2)}$ for (d) $\beta = 0.3$, $(e)\beta = 0.5$, (f) $\beta = 0.7$.

3.4 Conclusion

This research has presented the two layer flow of Newtonian and viscoelastic Ellis fluid under thermal and buoyancy effect with heat source. The mathematical models are simplified by lubrication approach and results are displayed through graphs and following observations are noted for velocity, pressure, temperature and stream function.

- The axial flow of Ellis fluid in both layers decays for the fluid viscosity $\mu^{(1)}$ and $\mu^{(2)}$.
- The axial flow of Newtonian and Ellis fluid rises by the heat radiation, buoyancy force and convection.
- The temperature of Newtonian and Ellis fluid rises by the radiation and convection.
- The pressure gradient in Newtonian fluid rises by the volumetric flow rate and buoyancy parameter but for Ellis fluid pressure gradient decays due to buoyancy parameter.

3.5 Appendix

$$
\begin{aligned}
f_1 &= \frac{c^{(2)}}{\mu^{(2)}}\left(1-\frac{\beta c^{(2)}}{\mu^{(2)}}\right)(h_1-h) \\
f_2 &= \frac{\beta}{3}\left(\frac{y^3-h_1^3}{{\mu^{(1)}}^2}-\frac{h_1^3-h^3}{{\mu^{(2)}}^2}\right) \\
f_3 &= \frac{y^2-h_1^2}{2\mu^{(1)}}+\frac{h_1^2-h^2}{2\mu^{(2)}}+\beta Gr_t\left(\begin{array}{c}\frac{-2B^{(1)}}{3}\left(\frac{y^3-h_1^3}{{\mu^{(1)}}^2}\right)+\frac{\Pr b}{15}\left(\frac{y^5-h_1^5}{{\mu^{(1)}}^2}\right) \\ \frac{-c^{(2)}}{Gr_t}\left(\frac{h_1^2-h^2}{{\mu^{(2)}}^2}\right)+\frac{2B^{(2)}}{3}\left(\frac{h_1^3-h^3}{{\mu^{(2)}}^2}\right)+ \\ \frac{A^{(2)}}{4}\left(\frac{h_1^4-h^4}{{\mu^{(2)}}^2}\right)-\frac{\Pr b}{15}\left(\frac{h_1^5-h^5}{{\mu^{(2)}}^2}\right)\end{array}\right) \\
f_4 &= -B^{(1)}\left(\frac{y^2-h_1^2}{2\mu^{(1)}}\right)+\frac{\Pr b}{24}\left(\frac{y^4-h_1^4}{\mu^{(1)}}\right)+\frac{\Pr b}{24}\left(\frac{h_1^4-h^4}{\mu^{(2)}}\right)-\frac{A^{(2)}}{6}\left(\frac{h_1^3-h^3}{\mu^{(2)}}\right)-B^{(2)}\left(\frac{h_1^2-h^2}{2\mu^{(2)}}\right) \\
f_5 &= \begin{array}{c}\frac{{B^{(1)}}^2 Gr_t}{3}\left(\frac{y^3-h_1^3}{{\mu^{(1)}}^2}\right)-\frac{B^{(1)}Gr_t\Pr b}{15}\left(\frac{y^5-h_1^5}{{\mu^{(1)}}^2}\right)+\frac{\Pr b}{42}\left(\frac{y^7-h_1^7}{{\mu^{(1)}}^2}\right)+B^{(2)}c^{(2)}\left(\frac{h_1^2-h^2}{{\mu^{(2)}}^2}\right) \\ +\frac{-{B^{(2)}}^2 Gr_t+A^{(2)}c^{(2)}}{3}\left(\frac{h_1^3-h^3}{{\mu^{(2)}}^2}\right)-\frac{3B^{(2)}Gr_tA^{(2)}+\Pr bc^{(2)}}{12}\left(\frac{h_1^4-h^4}{{\mu^{(2)}}^2}\right)+ \\ \frac{4B^{(2)}Gr_t\Pr b-3{A^{(2)}}^2 Gr_t}{60}\left(\frac{h_1^5-h^5}{{\mu^{(2)}}^2}\right)+\frac{A^{(2)}Gr_t\Pr b}{36}\left(\frac{h_1^6-h^6}{{\mu^{(2)}}^2}\right)-\frac{Gr_t\Pr^2 b^2}{252}\left(\frac{h_1^7-h^7}{{\mu^{(2)}}^2}\right)\end{array} \\
f_6 &= \frac{\partial u(h)}{\partial x}(y-h) \\
f_7 &= \frac{\beta}{3}\left(\frac{-h_1^3y+\frac{3h_1^4}{4}+\frac{y^4}{4}}{{\mu^{(1)}}^2}-\frac{h_1^3y+\frac{3h_1^4}{4}-h^3y-\frac{3h^4}{4}}{{\mu^{(2)}}^2}\right) \\
f_8 &= \frac{\frac{h_1^3}{3}-\frac{h_1^2y}{2}+\frac{y^3}{6}}{\mu^{(1)}}+\frac{h_1^2y-\frac{2h_1^3}{3}-h^2y+\frac{2h^3}{3}}{2\mu^{(2)}} \\
f_9 &= \begin{array}{c}\frac{-2B^{(1)}}{3}\left(\frac{-h_1^3y+\frac{3h_1^4}{4}+\frac{y^4}{4}}{{\mu^{(1)}}^2}\right)+\Pr b\left(\frac{\frac{-h_1^5y}{15}+\frac{h_1^6}{18}+\frac{y^6}{90}}{{\mu^{(1)}}^2}\right)-\frac{c^{(2)}}{Gr_t}\left(\frac{h_1^2y-\frac{2h_1^3}{3}-h^2y+\frac{2h^3}{3}}{{\mu^{(2)}}^2}\right)+ \\ \frac{2B^{(2)}}{3}\left(\frac{h_1^3y+\frac{3h_1^4}{4}-h^3y-\frac{3h^4}{4}}{{\mu^{(2)}}^2}\right)+\frac{A^{(2)}}{4}\left(\frac{h_1^4y-\frac{4h_1^5}{5}-h^4y+\frac{4h^5}{5}}{{\mu^{(2)}}^2}\right)-\frac{\Pr b}{15}\left(\frac{h_1^5y-\frac{5h_1^6}{6}-h^5y+\frac{5h^6}{6}}{{\mu^{(2)}}^2}\right)\end{array} \\
f_{10} &= u(h)(y-h)
\end{aligned}
$$

$$
\begin{array}{rcl}
f_{11} & = & \begin{array}{c}
\frac{-B^{(1)}}{2\mu^{(1)}}\left(\frac{y^3}{3}-h_1^2y\right)+\frac{\Pr b}{24\mu^{(1)}}\left(\frac{y^5}{5}-h_1^4y\right)+\frac{\Pr b}{24}\left(\frac{h_1^4-h^4}{\mu^{(2)}}\right)y \\
-\frac{A^{(2)}}{6}\left(\frac{h_1^3-h^3}{\mu^{(2)}}\right)y-\frac{B^{(2)}}{2}\left(\frac{h_1^2-h^2}{\mu^{(2)}}\right)y+ \\
\beta\left(\begin{array}{c}
\frac{{B^{(1)}}^2 Gr_t}{3{\mu^{(1)}}^2}\left(\frac{y^4}{4}-h_1^3y\right)-\frac{B^{(1)}Gr_t\Pr b}{15{\mu^{(1)}}^2}\left(\frac{y^6}{6}-h_1^5y\right)+ \\
\frac{\Pr b}{42{\mu^{(1)}}^2}\left(\frac{y^8}{8}-h_1^7y\right)+\frac{B^{(2)}c^{(2)}y}{{\mu^{(2)}}^2}\left(h_1^2-h^2\right)+ \\
\frac{-Gr_t{B^{(2)}}^2+A^{(2)}c^{(2)}}{3}\left(\frac{h_1^3-h^3}{{\mu^{(2)}}^2}\right)y-\frac{3Gr_tB^{(2)}A^{(2)}+\Pr bc^{(2)}}{12}\left(\frac{h_1^4-h^4}{{\mu^{(2)}}^2}\right)y+ \\
\frac{4Gr_tB^{(2)}\Pr b-3{A^{(2)}}^2Gr_t}{60}\left(\frac{h_1^5-h^5}{{\mu^{(2)}}^2}\right)y+\frac{Gr_t\Pr bA^{(2)}y}{36}\left(\frac{h_1^6-h^6}{{\mu^{(2)}}^2}\right)- \\
\frac{Gr_t\Pr^2b^2y}{252}\left(\frac{h_1^7-h^7}{{\mu^{(2)}}^2}\right)
\end{array}\right)
\end{array} \\
f_{12} & = & \frac{c^{(2)}}{2\mu^{(2)}}\left(1-\frac{\beta c^{(2)}}{\mu^{(2)}}\right)\left(h_1^2-h^2\right) \\
f_{13} & = & \left[\begin{array}{c}
\frac{B^{(1)}}{3}\frac{h_1^3}{\mu^{(1)}}-\frac{\Pr b}{30}\frac{h_1^5}{\mu^{(1)}}+\frac{\Pr b}{30\mu^{(2)}}\left(h_1^5-h^5\right)- \\
\frac{A^{(2)}}{8\mu^{(2)}}\left(h_1^4-h^4\right)-\frac{B^{(2)}}{3\mu^{(2)}}\left(h_1^3-h^3\right)+ \\
\beta\left(\begin{array}{c}
\frac{-{B^{(1)}}^2Gr_t}{4}\frac{h_1^4}{{\mu^{(1)}}^2}-\frac{\Pr b}{48}\frac{h_1^8}{{\mu^{(1)}}^2}+\frac{B^{(1)}Gr_t\Pr b}{18}\frac{h_1^6}{{\mu^{(1)}}^2}+ \\
\frac{2B^{(2)}c^{(2)}}{3{\mu^{(2)}}^2}\left(h_1^3-h^3\right)+\frac{-Gr_t{B^{(2)}}^2+A^{(2)}c^{(2)}}{4{\mu^{(2)}}^2}\left(h_1^4-h^4\right)- \\
\frac{3Gr_tB^{(2)}A^{(2)}+\Pr bc^{(2)}}{15{\mu^{(2)}}^2}\left(h_1^5-h^5\right)+\frac{4Gr_tB^{(2)}\Pr b-3Gr_t{A^{(2)}}^2}{72{\mu^{(2)}}^2}\left(h_1^6-h^6\right)+ \\
\frac{Gr_tA^{(2)}\Pr b}{42{\mu^{(2)}}^2}\left(h_1^7-h^7\right)-\frac{Gr_t\Pr^2b^2}{288{\mu^{(2)}}^2}\left(h_1^8-h^8\right)
\end{array}\right)
\end{array}\right] \\
g_1 & = & \frac{c^{(2)}}{\mu^{(2)}}\left(1-\frac{\beta c^{(2)}}{\mu^{(2)}}\right)(y-h) \\
g_2 & = & \frac{-\beta}{3}\left(\frac{y^3-h^3}{{\mu^{(2)}}^2}\right) \\
g_3 & = & \left[\frac{1}{2}\left(\frac{y^2-h^2}{\mu^{(2)}}\right)+\frac{\beta Gr_t}{\mu^{(2)}}\left(\begin{array}{c}
\frac{-c^{(2)}}{Gr_t}\left(\frac{y^2-h^2}{\mu^{(2)}}\right)+\frac{2B^{(2)}}{3}\left(\frac{y^3-h^3}{\mu^{(2)}}\right)+ \\
\frac{A^{(2)}}{4}\left(\frac{y^4-h^4}{\mu^{(2)}}\right)-\frac{\Pr b}{15}\left(\frac{y^5-h^5}{\mu^{(2)}}\right)
\end{array}\right)\right] \\
g_4 & = & \frac{\Pr b}{24}\left(\frac{y^4-h^4}{\mu^{(2)}}\right)-\frac{A^{(2)}}{6}\left(\frac{y^3-h^3}{\mu^{(2)}}\right)-\frac{B^{(2)}}{2}\left(\frac{y^2-h^2}{\mu^{(2)}}\right) \\
g_5 & = & \left[\begin{array}{c}
-B^{(2)}c^{(2)}\left(\frac{y^2-h^2}{\mu^{(2)}}\right)-\frac{A^{(2)}c^{(2)}}{3}\left(\frac{y^3-h^3}{\mu^{(2)}}\right)+\frac{c^{(2)}\Pr b}{12}\left(\frac{y^4-h^4}{\mu^{(2)}}\right)+ \\
Gr_t\left(\begin{array}{c}
\frac{{B^{(2)}}^2}{3}\left(\frac{y^3-h^3}{\mu^{(2)}}\right)+\frac{A^{(2)}B^{(2)}}{4}\left(\frac{y^4-h^4}{\mu^{(2)}}\right)+\frac{{A^{(2)}}^2}{20}\left(\frac{y^5-h^5}{\mu^{(2)}}\right)- \\
\frac{\Pr bB^{(2)}}{15}\left(\frac{y^5-h^5}{\mu^{(2)}}\right)-\frac{\Pr bA^{(2)}}{36}\left(\frac{y^6-h^6}{\mu^{(2)}}\right)+\frac{\Pr^2b^2}{252}\left(\frac{y^7-h^7}{\mu^{(2)}}\right)
\end{array}\right)
\end{array}\right] \\
g_6 & = & \frac{-\beta}{3{\mu^{(2)}}^2}\left(\frac{y^4}{4}-h^3y+\frac{3h^4}{4}\right) \\
g_7 & = & \frac{1}{2}\left(\frac{y^3}{3}-h^2y+\frac{2h^3}{3}\right)
\end{array}
$$

$$g_8 = \frac{-c^{(2)}}{Gr_t}\left(\frac{y^3}{3}-h^2y+\frac{2h^3}{3}\right)+\frac{2B^{(2)}}{3}\left(\frac{y^4}{4}-h^3y+\frac{3h^4}{4}\right)+\frac{A^{(2)}}{4}\left(\frac{y^5}{5}-h^4y+\frac{4h^5}{5}\right)- \frac{\Pr b}{15}\left(\frac{y^6}{6}-h^5y+\frac{5h^6}{6}\right)$$

$$g_9 = \frac{c^{(2)}}{\mu^{(2)}}\left(1-\frac{\beta c^{(2)}}{\mu^{(2)}}\right)\left(\frac{y^2}{2}-hy\right)$$

$$g_{10} = \frac{\Pr b}{24}\left(\frac{y^5}{5}-h^4y\right)-\frac{A^{(2)}}{6}\left(\frac{y^4}{4}-h^3y\right)-\frac{B^{(2)}}{2}\left(\frac{y^3}{3}-h^2y\right)$$

$$g_{11} = \left[\begin{array}{c} -B^{(2)}c^{(2)}\left(\frac{y^3}{3}-h^2y\right)-\frac{A^{(2)}c^{(2)}}{3}\left(\frac{y^4}{4}-h^3y\right)+\frac{c^{(2)}\Pr b}{12}\left(\frac{y^5}{5}-h^4y\right)+ \\ Gr_t\left(\begin{array}{c} \frac{{B^{(2)}}^2}{3}\left(\frac{y^4}{4}-h^3y\right)+\frac{A^{(2)}B^{(2)}}{4}\left(\frac{y^5}{5}-h^4y\right)+\frac{{A^{(2)}}^2}{20}\left(\frac{y^6}{6}-h^5y\right)- \\ \frac{\Pr bB^{(2)}}{15}\left(\frac{y^6}{6}-h^5y\right)-\frac{A^{(2)}\Pr b}{36}\left(\frac{y^7}{7}-h^6y\right)+\frac{\Pr^2 b^2}{252}\left(\frac{y^8}{4}-h^7y\right) \end{array}\right) \end{array}\right]$$

$$g_{12} = \beta\left(\frac{-h_1^4}{4{\mu^{(1)}}^2}-\frac{h_1^4-h^3h_1}{3{\mu^{(2)}}^2}+\left(\frac{h^4}{4{\mu^{(2)}}^2}+\frac{h_1^4}{12{\mu^{(2)}}^2}-\frac{h^3h_1}{3{\mu^{(2)}}^2}\right)\right)$$

$$g_{13} = \beta Gr_t\left(\begin{array}{c} \frac{1}{2}\left(\frac{-2h_1^3}{3\mu^{(1)}}+\frac{h_1^3-h^2h_1}{\mu^{(2)}}\right)+\frac{1}{\mu^{(2)}}\left(\frac{-h^3}{3}-\frac{h_1^3}{6}+\frac{h^2h_1}{2}\right)+ \\ \frac{B^{(1)}h_1^4}{2{\mu^{(1)}}^2}-\frac{\Pr bh_1^6}{18{\mu^{(1)}}^2}-\frac{c^{(2)}\left(h_1^3-h^2h_1\right)}{Gr_t{\mu^{(2)}}^2}+\frac{2B^{(2)}\left(h_1^4-h^3h_1\right)}{3{\mu^{(2)}}^2}+\frac{A^{(2)}\left(h_1^5-h^4h_1\right)}{4{\mu^{(2)}}^2} \\ -\frac{\Pr b\left(h_1^6-h^5h_1\right)}{15{\mu^{(2)}}^2}-\frac{c^{(2)}}{2Gr_t\mu^{(2)}}\left(\frac{1}{\mu^{(2)}}\left(\frac{-h^3}{3}-\frac{h_1^3}{6}+\frac{h^2h_1}{2}\right)\right)- \\ 2B^{(2)}\left(\frac{h^4}{4{\mu^{(2)}}^2}+\frac{h_1^4}{12{\mu^{(2)}}^2}-\frac{h^3h_1}{3{\mu^{(2)}}^2}\right)+\frac{A^{(2)}}{4{\mu^{(2)}}^2}\left(\frac{-4h^5}{5}-\frac{h_1^5}{5}+h^4h_1\right)- \\ \frac{\Pr b}{15{\mu^{(2)}}^2}\left(\frac{-5h^6}{6}-\frac{h_1^6}{6}+h^5h_1\right) \end{array}\right)$$

Bibliography

[1] Maqbool K, Manzoor N, Ellahi R, Sait SM. Influence of heat transfer on MHD Carreau fluid flow due to motile cilia in a channel. Journal of Thermal Analysis and Calorimetry. 2021 Jun;144:2317-26.

[2] Sadaf H, Nadeem S. Fluid flow analysis of cilia beating in a curved channel in the presence of magnetic field and heat transfer. Canadian Journal of Physics. 2020 Jan;28;98(2):191-7.

[3] Akbar NS, Muhammad T. Physical aspects of electro osmotically interactive Cilia propulsion on symmetric plus asymmetric conduit flow of couple stress fluid with thermal radiation and heat transfer. Scientific Reports. 2023 Oct 28;13(1):18491.

[4] Akbar NS, Khan ZH, Nadeem S. Metachronal beating of cilia under influence of Hartmann layer and heat transfer. The European Physical Journal Plus. 2014 Aug 22;129:1-9.

[5] Imran A, Raja MA, Shoaib M, Zeb M, Nisar KS. Electro-osmotic transport of a Williamson fluid within a ciliated microchannel with heat transfer analysis. Case Studies in Thermal Engineering. 2023 May 1;45:102904.

[6] Bhatti MM, Ishtiaq F, Ellahi R, Sait SM. Novel aspects of cilia-driven flow of viscoelastic fluid through a non-darcy medium under the influence of an induced magnetic field and heat transfer. Mathematics. 2023 May 14;11(10):2284.

[7] Mills ZG, Aziz B, Alexeev A. Beating synthetic cilia enhance heat transport in microfluidic channels. Soft Matter. 2012 Sep 20;8(45):11508-13.

[8] Butt AW, Akbar NS, Mir NA. Heat transfer analysis of peristaltic flow of a Phan-Thien–Tanner fluid model due to metachronal wave of cilia. Biomechanics and Modeling in Mechanobiology. 2020 Oct;19:1925-33.

[9] Rafiq M, Shaheen S, Khan MI, Fadhl BM, Hassine SB, ElDin SM. Impact of ciliated walls on peristaltic flow of Rabinowitsch fluid through flexible tube with heat/mass transfer. Case Studies in Thermal Engineering. 2023 May 1;45:102990.

[10] Akbar NS, Butt AW. Heat transfer analysis of viscoelastic fluid flow due to metachronal wave of cilia. International Journal of Biomathematics. 2014 Nov 15;7(06):1450066.

[11] Rajashekhar C, Manjunatha G, Prasad KV, Divya BB, Vaidya H. Peristaltic transport of two-layered blood flow using Herschel–Bulkley Model. Cogent Engineering. 2018 Jan 1;5(1):1495592.

[12] Ashraf H, Siddique I, Siddiqa A, Tawfiq FM, Tchier F, Zulqarnain RM, Rehman HU, Bhatti S, Rehman A. Analysis of two layered peristaltic-ciliary transport of Jeffrey fluid and in vitro preimplantation embryo development. Scientific Reports. 2024 Jan 17;14(1):1469.

[13] Fatima N, Nisar KS, Shaheen S, Arain MB, Ijaz N, Muhammad T. A case study for heat and mass transfer of viscous fluid flow in double layer due to ciliated channel. Case Studies in Thermal Engineering. 2023 May 1;45:102943.

[14] Asghar Z, Khan MW, Shatanawi W, Gondal MA. Semi-analytical solution of Graetz–Brinkman problem combined with non-Newtonian Ellis fluid flow in a passive channel. The European Physical Journal Plus. 2023 Nov 1;138(11):978.

[15] Channakote MM, Siddabasappa C, Tripathi D. Peristaltic mechanism of Ellis fluid with viscous dissipation and thermal radiation induced by cilia wave. International Journal of Computational Materials Science and Engineering. 2024 Mar 21:2450006.

[16] Shaheen S, Huang H, Al-Yarimi FA, Arain MB. Theoretical analysis of Ellis fluid flow in two layers due to metachronal propulsion subject to heat and mass transfer: Application in biological function. Case Studies in Thermal Engineering. 2024 Jul 1;59:104446.

[17] Asghar Z, Khalid U, Nazeer M, Rasheed HS, Kausar A. Computational study of flow and heat transfer analysis of Ellis fluid model in complicated divergent channel. Modern Physics Letters B. 2024 May 20;38(14):2450119.

[18] Abbasi A, Khan SU, Farooq W, Mughal FM, Khan MI, Prasannakumara BC, El-Wakad MT, Guedri K, Galal AM. Peristaltic flow of chemically reactive Ellis fluid through an asymmetric channel: Heat and mass transfer analysis. Ain Shams Engineering Journal. 2023 Feb 1;14(1):101832.

[19] Ali N, Kazmi HR, Ullah K. A study on the bifurcation of the peristaltic driven flow of Ellis fluid. Waves in Random and Complex Media. 2023 Feb 22:1-8.

[20] Javed M, Qadeer F, Imran N, Kumam P, Sohail M. Peristaltic mechanism of Ellis fluid in curved configuration with homogeneous and heterogeneous effects. Alexandria Engineering Journal. 2022 Dec 1;61(12):10677-88.

[21] Nadeem S, Akbar NS. Effects of heat transfer on the peristaltic transport of MHD Newtonian fluid with variable viscosity: application of Adomian decomposition method. Communications in Nonlinear Science and Numerical Simulation. 2009 Nov 1;14(11):3844-55.